PROCEDURE FOR THE SHEAR ANALYSIS OF THIN-WALLED METAL CYLINDERS SUBJECTED TO BENDING AND TORSIONAL LOADS

By

John J. Reid

Bachelor of Science

University of New Mexico

Albuquerque, New Mexico

1951

Submitted to the Faculty of the Graduate School of
the Oklahoma State University in partial
fulfillment of the requirements
for the degree of
MASTER OF SCIENCE
August, 1957

PROCEDURE FOR THE SHEAR ANALYSIS OF THIN-WALLED METAL CYLINDERS SUBJECTED TO BENDING AND TORSIONAL LOADS

Report approved:

_____
Report Adviser

_____

_____

_____
Dean of Graduate School

PREFACE

Recently, while employed as a stress analyst for an airframe manufacturer, the author became interested in the load-carrying capabilities of thin-walled stiffened cylinders such as airplane wings and other types of thin-walled structures which result from the requirement that heavy loads be resisted by the lightest possible structure. An evaluation by the author of his training and experience in what may be termed "civil engineering structures" indicated a sound basis for analytical work with aircraft structures, but also pointed out the need for acquiring knowledge of the behavior of structures common to the airplane and the methods used to analyze them.

Since the determination of the shearing stresses is of particular interest to the author, and since shearing stresses are required as a preliminary part of a complete analysis of a structure, this subject was chosen for first study. The study was begun with the rudiments of the shear analysis of various shaped thin-walled structures without stiffening members, and progressed through a procedure for the shear analysis of an airplane wing. This report records the results of this study.

The author wishes to express his gratitude to Lloyd Jackson and William Burkitt of the Stress Analysis Group of Douglas Aircraft Co., Inc., Tulsa Division, and to Professor Raymond E. Chapel for their technical assistance; to Roger L. Flanders, Professor and Head of the School of Civil Engineering, and to Professor Jan J. Tuma who have read the complete manuscript, made many valuable suggestions, and given freely of

their time to the author during the preparation of this report; to Douglas Aircraft Co., Inc., for making the author's graduate study possible; to the Tulsa Division of this company, and to the National Advisory Committee for Aeronautics, Washington, D. C., for making available documents used during the study; and finally to the author's wife, without whose help and understanding, the author's graduate study would not be feasible.

TABLE OF CONTENTS

LIST OF ILLUSTRATIONS

Figure Page

NOMENCLATURE

A	Area in square inches; Coefficient.
B, C, K, N.	Coefficients.
D	Diameter of cylinder in inches; Coefficient.
E	Modulus of elasticity in pounds per square inch; Coefficient.
F	Force in pounds.
$F_{C_{CR}}$	Compressive stress at instant of crippling, pounds per sq. in.
G	Modulus of rigidity in pounds per square inch; Coefficient.
H	Height above the cross-section of a hollow cylinder of the plane which represents St. Venant's stress function for the hollow portion of the cylinder; Coefficient.
I	Moment of inertia of an area in $(\text{inches})^4$. Subscripts x and y designate bending axes. Subscript p designates polar moment of inertia.
L	Length in inches; Coefficient.
M	Bending or torsional moment of forces; Coefficient.
P	Force on stringer in pounds.
R, r	Radial distance in inches.
T	Torsional moment in inch-pounds.
U	Strain energy in inch-pounds.
V	Vertical shearing force in pounds. Subscripts w and f designate web and flange, respectively.
X_{RS}	Distance along the rear spar of an airplane wing from a fixed origin in inches.

X, Y, Z	Designates mutually perpendicular bending axes.
C. G.	Center of gravity of areas of the structural elements of a cross-section.
a, b, d h, y	Distance in inches
c	Distance from the bending axis to the extreme fibre in inches; Distance in inches.
f_b	Bending stress in pounds per square inch.
f_s	Shearing stress in pounds per square inch.
f_{st}	Stringer average stress in pounds per square inch.
f_{yp}	Yield point stress in pounds per square inch.
ℓ	Distance between stringers along the shell in inches.
q'	Relative shear flow from bending in pounds per inch.
q_o	Unknown shear flow at a specific point in pounds per inch.
q_1, q_2, q_3	Unknown constant shear flows in cells 1, 2, and 3, respectively.
t	Thickness of metal shell or web in inches.
u_1, u_2	Angular measurement in degrees.
w	Effective width of shell each side of a stringer attachment line in inches.
ds	Elemental distance along the periphery of a cell in inches.
Δ	Designates a change in a quantity or a difference in the same quantity measured at two points.
θ	Angular deformation of a cell in degrees or radians.
μ	Poison's ratio.
α, β	Angular measurements in degrees or radians.
ρ	Moment arm or distance in inches.

φ Symbol for St. Venant's stress function.

Sign convention:

Clockwise shear flows are positive.

Bending moments causing tension in lower extreme fibre are positive.

Distances measured forward from the rear spar of a wing cross-section are negative.

Distances measured downward from the Y-axis in the wing cross-section are negative.

PART 1

INTRODUCTION

To study the action, under load, of the complicated thin-walled structures common to aircraft, an understanding of the basic theory and analytical tools available for the analysis of the elements of these structures must be gained. This information is available in standard texts on aircraft structures, such as Bruhn (1949) and Peery (1950). As the elements of the structure are assembled, the number of analytical tools necessary will be increased and new procedures for the analysis will be developed.

This report will show the origin of the necessary basic theory and procedures for the determination of the shearing stresses in thin-walled structures of varying degrees of complexity. The ultimate goal will be to show the procedures for the determination of the shearing stresses of a multi-cell, multi-stiffener, thin-walled structure.

Whenever reports of structural tests are available - particularly for a type of structure with which the interested engineer is not thoroughly familiar - they should be examined with a view to obtaining information of the behavior of the structure under load, and, perhaps more important, to attempt to obtain a "feeling" or degree of intuition regarding the behavior of the structure under load. Some of the more informative test reports regarding thin-walled cylinders which are available from the National Advisory Committee for Aeronautics, Wash-

ington, D. C. are included in the bibliography. Since the research and testing programs reported upon by the aforementioned documents have for their ultimate aim the examination of the tested structure at or near failure, very little effort is spent deriving theory of a basic nature regarding the structure when the stresses are such that the structure does not assume any inelastic deformation. However, among some of the things which can be observed from the curves, graphs and photograph reproductions of the tested structures during various phases of loading are the following: the build-up of stresses during test, the point where inelastic deformation takes place, and the effect of varying the stiffener spacing and other dimensional ratios.

Since the assumption is made throughout the report that the structure examined behaves elastically and does not buckle, the theory noted and the procedures for analysis shown are valid for elastic behavior only. However, in aircraft practice, since no main part of the structure is allowed to assume inelastic deformation under the loads actually imposed on it, the procedure shown in this report for single and multi-cell thin-walled structures is acceptable. Some of these procedures are in use by airframe manufacturers.

PART II

A SYNOPSIS OF ST. VENANT'S PRINCIPLE REGARDING THE TORSIONAL SHEARING STRESSES IN THIN-WALLED CYLINDERS

In St. Venant's analysis of the torsion of solid prismatic bars of non-circular cross-section, there can be found a stress function φ such that $\frac{\partial^2 \varphi}{\partial x^2} + \frac{\partial^2 \varphi}{\partial y^2} = -2G\frac{\Theta}{L}$ and $\varphi = 0$ along the boundary. The shearing stresses at any point in the bar are given by the derivatives of φ. $\tau_{zx} = \frac{\partial \varphi}{\partial y}$; $\tau_{zy} = -\frac{\partial \varphi}{\partial x}$. Also the volume beneath the surface representing the stress function is equal to 1/2 the twisting moment, $T = 2\iint \varphi \, dx \, dy$

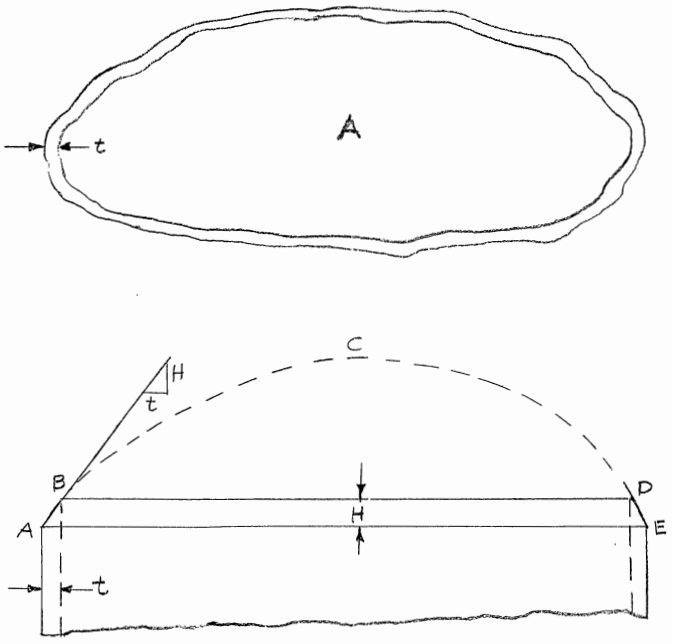

FIGURE 1

In Figure 1, let ABCDE be the cross-section of the surface representing the function φ for a hollow bar. Since the bar is hollow, the surface BCD extending over the hollow portion can have no physical significance, because stresses here do not exist. Hence the surface BCD must be replaced by a surface which has a slope of zero everywhere over the hollow portion. Such a surface is represented by the plane BD whose distance above the cross-section is H. The surface representing the stress function φ is therefore ABDE. The same use can now be made of the stress function represented by the surface ABDE in solving the problem of the torsional resistance of a hollow bar as was made of the function φ for a solid bar.

The twisting moment T to which the hollow bar is subjected is equal to twice the volume underneath the surface ABDE, and is therefore approximately

$$T = 2AH \qquad (1)$$

where A is approximately the inside area of the hollow section (or the area within the mean perimeter) and H is the height of the plane BD above the cross-section. It must be emphasized that the above formula holds only for thin-walled sections.

The approximation involves the assumption that the torsional shearing stress is constant over the thickness of the wall, an assumption which is common in dealing with the torsional resistance of thin-walled sections. The slope of the surface at any point is equal to the stress in the bar in a direction perpendicular to the direction in which the slope is taken. Hence, if the wall of the hollow bar is relatively thin, the slope at any point along the arcs AB or DE may be taken, without serious error, as H/t where t is the wall thickness. The shearing

stress in the bar is therefore

$$\tau = H/t$$

$$\text{But } H = \frac{T}{2A}$$

$$\text{Therefore } \tau = \frac{T}{2At} \qquad (2)$$

In some applications of thin-walled members subjected to shearing stresses, it is more convenient to use an expression for the shear flow q instead of that for the torsional shearing stress τ. By definition $q = \tau t$. Then $q = \frac{T}{2A}$, (2a)

It should be noted that the quantity H is equal to the shear flow q. The equation $\tau = \frac{T}{2At}$ may be used in calculating the stresses in tubular members under torsion prior to buckling if the thickness of the wall is small, variations in thicknesses are not abrupt, and there are no re-entrant corners. (Timoshenko, 1956, Pg. 248). These, then, are the assumptions which are made when using equation (2) or (2a).

It is very difficult to apply the Soap-Film Analogy as an expermental tool when concerned with thin-walled hollow sections. However, one of the major benefits of the Soap-Film Analogy is as an aid in the visualization of the comparative magnitude of the stresses in the section. This can be understood from the fact that the shearing stresses are proportional to the slope of the stretched membrane (analogous to the stress function φ). The Soap-Film Analogy will apply to hollow bars if the opening representing the cross-section has the inside boundary raised a distance H above the outside boundary, as is shown in Figure 1.

The equation for the shear flow due to torsion in thin-walled sec-

tions, $q = \frac{T}{2A}$, can be derived without the aid of St. Venant's principle as follows:

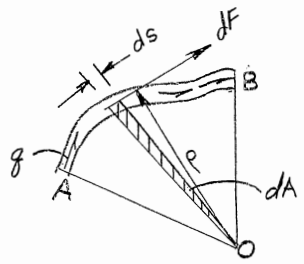

FIGURE 2

The above figure represents a portion of the thin-walled tube shown in Figure 1. O is any point, ρ is the moment arm about O of the force dF, and q is the constant shear flow (f_s t).

$$dF = qds \qquad dT = 2qdA$$

$$dT = \rho\, qds \qquad T = 2q \int dA$$

$$dA = 1/2\ \rho\, ds \qquad = 2qA$$

$$dT = 2\rho \frac{dA}{q\rho} \qquad q = \frac{T}{2A} \qquad (2a)$$

where A is the area enclosed by the mean perimeter of the closed cross-section, and $f_s = \tau$ = shearing stress.

That the shear flow q produced by pure torsion of a thin-walled closed section is constant around the walls of the cross-section may be shown with reference to Figure 3. Let any two longitudinal sections, 1-1' and 2-2', be taken in the general thin-walled member of Figure 3 subjected to torsion only. The length of section 1-1' equals the length of section 2-2' equals L.

The sum of the forces in a longitudinal direction equals zero.

$$q_1 L + q_2 L = 0$$

$$|q_1| = |q_2|$$

$$\Sigma M_{1'} = 0$$

$$q_1 L d + q L d = 0$$

$$|q_1| = |q|$$

$$q_1 = q_2 = q$$

The shear flows are equal at points 1 and 2.

It may be noted that the shear flow $q = f_s t$ may be obtained before the shear stress is determined.

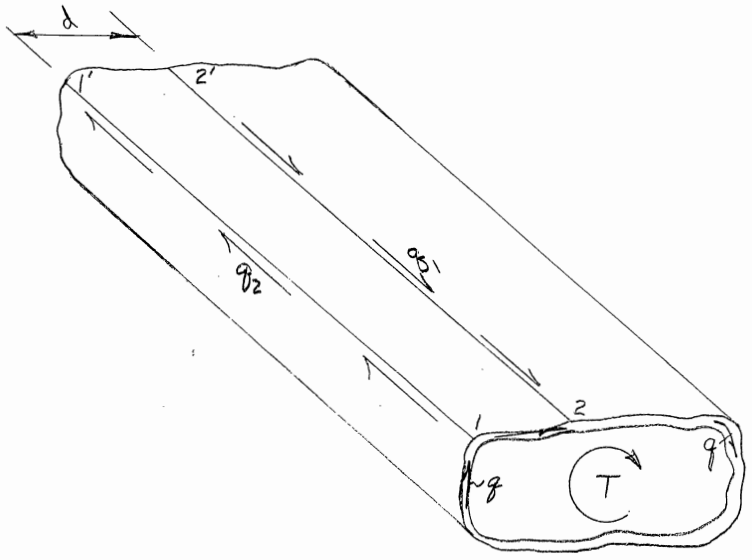

FIGURE 3

PART III

SHEARING STRESSES IN HOLLOW THIN-WALLED BEAMS

DUE TO BENDING FROM A VERTICAL FORCE

The thin-walled hollow beam shown in Figure 4 will be considered.

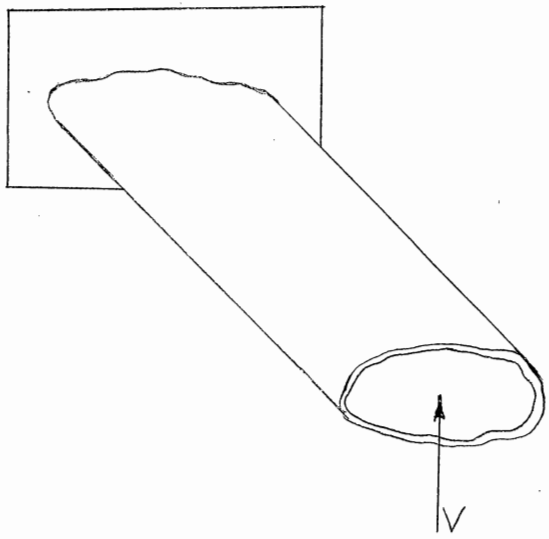

FIGURE 4

The shearing force V parallel to the beam cross-section produces a shearing stress f_s of varying intensity over the area of the cross-section. Since the shearing stresses on any two perpendicular planes are equal, the shearing stresses on any horizontal plane through the beam are equal to the vertical shearing stresses on the cross-section at the point of intersection of the two planes. Then the magnitude of the vertical shearing stresses at any point on the cross-section will be obtained if the horizontal shearing stresses at the point are

computed.

Consider a portion of the beam between two vertical cross-sections, held in equilibrium by the forces and moments shown in Figure 5. At this point in the discussion, assume the line of action of V such as to produce no torsion nor unsymmetrical bending on the beam shown. Also assume that the cross-section of the beam remains constant along its length. The effects on the shearing stress of these restrictions will be discussed at the end of this section.

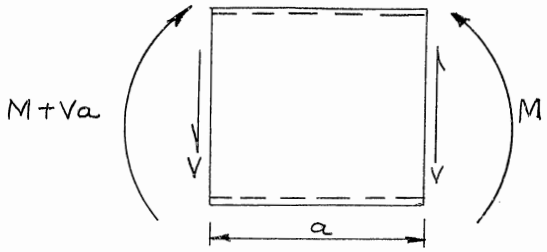

FIGURE 5

The shearing forces V will be equal in magnitude and opposite in direction. The bending moment on the cross-section to the left will be M + Va, where M is the bending moment on the right cross-section. Provided the portion of the beam does not buckle or yield, the stress situation will be as shown by Figure 6.

At a point a distance y from the neutral axis the bending stress will be $\frac{My}{I}$ on the right face and $\frac{My}{I} + \frac{Vay}{I}$ on the left face. In order to obtain the shearing stress at a distance y_1 above the neutral axis, the portion of the beam above this point will be considered as a free body as shown in Figure 6 (2). The resultant force on the cross-

section on the left is greater than that on the right. For equilibrium of horizontal forces, the forces produced by the shearing stresses f_s on the horizontal area of width b and length a must be equal to the differences in the normal forces on the two cross-sections.

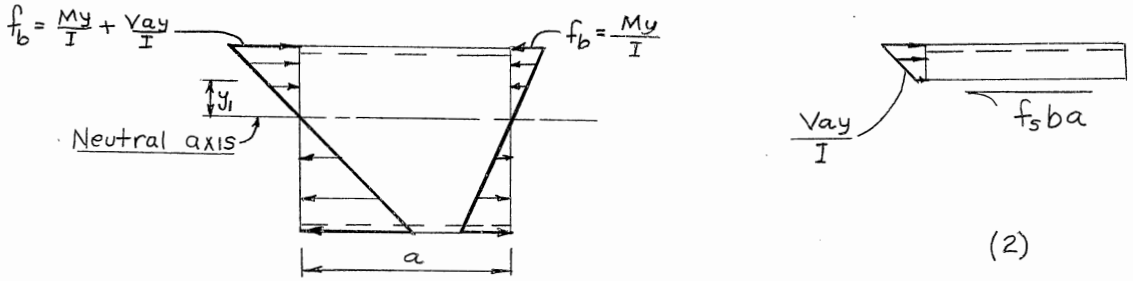

FIGURE 6

Since only the differences in the forces need be considered, the loading shown in Figure 6 (2) may be used in computing the shearing stresses.

$$\Sigma F_H = 0$$

$$f_s ba = \int_{y_1}^{c} \frac{Vay}{I} dA$$

$$f_s = \frac{V}{Ib} \int_{y_1}^{c} y\, dA \qquad (3)$$

where the integral represents the static moment of the area of the cross-section above y_1, the point at which the shearing stress is desired, and b is the sum of the wall thicknesses along a horizontal plane at the distance y_1 from the neutral axis. The shearing stress

f_s in formula (3) is in a vertical direction and the dimension b is in a horizontal direction. Consider a point A on the left wall of a cross-section of Figure 4 a distance y_1 above the neutral axis. Let the thickness of the wall at point A in a horizontal direction be b_A and the corresponding thickness of the right wall be $b_{A'}$. $f_s b_A$ is a shearing force per inch of wall at point A and acts in a vertical direction. If α is the angle between the vertical direction and a tangent to the cross-section boundary at point A, $f_s b_A \cos \alpha$ will be a shearing force per inch of wall which is tangent to the cross-section boundary. $b_A \cos \alpha$ is the radial thickness of the wall at point A and can be called t_A. Then, the shear flow at point A tangent to the cross-section boundary will be given by the equation:

$$q = f_s t_A = \frac{V}{It_A} \int_{y_1}^{y_o} y dA \qquad (3a)$$

where y_o is the point of zero shear flow on the cross-section above point A. Since the shear flow at point A given by equation (3a) is tangent to the cross-section boundary, it may be combined algebraically with a shear flow at the same point due to torsion, if desired.

It was previously noted that in the above derivation of formula (3), no torsion was introduced. If the vertical shearing force V is applied at a point other than the shear center, there will be a torque T = Ve applied to the section, where e is the moment arm from the shear center to the vertical force V. An analogous situation is that of a force V and a couple T = Ve applied at the shear center. The effects of a torque applied to thin-walled closed sections was discussed in a previous section. The beam shear due to a vertical force V at the shear center was discussed in this section. By the method of superposition the shearing stress f_s or the shear flow q may be found.

The condition of unsymmetrical bending deserves further consideration. The simple beam formula applies only to special cases of beam flexure. The resultant bending moment on the cross-section must act about one of the principle axis of the area. The neutral axis will then be parallel to the axis of the resultant bending moment. In the more general cases of beam flexure, however, the resultant bending moment is not about one of the principal axes; then the direction of the neutral axis cannot be determined by inspection. One method of finding the beam shear, $f_s = \frac{V}{Ib} \int ydA$, when the vertical force V is applied to the cross-section at an angle other than 90° to the principle axis is to resolve the force V into components perpendicular to the principle axes and proceed as outlined in this section with each component in turn. The principle of superposition can be used to obtain the beam shearing stress at any point in the cross-section. If the cross-sections of the beam are not constant along its length, changes in the shearing stress from section to section may occur, and the shearing stress given by formula (3) may be considerably in error. For tapered beams, formula (3) may be used if the value V is replaced by a quantity kV, k depending on the dimensions of the taper.

PART IV

TORSIONAL SHEARING STRESSES IN THIN-WALLED CIRCULAR CYLINDERS

According to St. Venant's principal for torsion of bars, the torsional stress f_s in a hollow tube is given approximately by the expression $f_s = \frac{T}{2At}$ where T is the torsional moment on the section, A is the area enclosed by the mean perimeter and t is the wall thickness at the point where the stress is desired. For a circular thin-walled tube as shown in Figure 7, $A = \pi r^2$

$$f_s = \frac{T}{2\pi r^2 t} \qquad \left| \qquad q = \frac{T}{2\pi r^2} \right. \qquad (4)$$

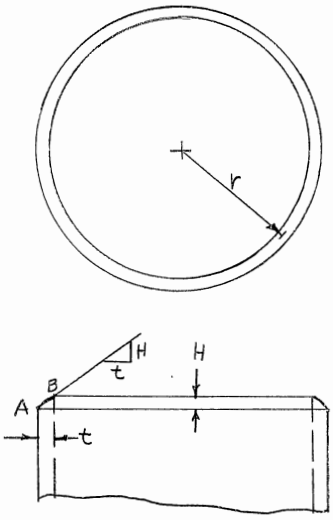

FIGURE 7

It may again be noted that the approximation involved in expression (4) arises from the assumption that the stresses are constant over the thickness of the wall (constant slope of membrane section AB). For wall thicknesses very small as compared to the diameter of the tube ($\frac{D}{t} > 50$), the formula gives excellent results. In the use of formula (4), it is further assumed that the tube, or cylinder, does not buckle and that the wall thickness does not change abruptly around the cross-section.

PART V

SHEARING STRESSES IN A THIN-WALLED CIRCULAR TUBE DUE TO BENDING FROM A VERTICAL FORCE

As stated previously, a vertical shearing force parallel to the beam cross-section produces a shearing stress of varying intensity over the cross-section. This shearing stress is given by the expression

$$f_s = \frac{V}{Ib} \int ydA$$

The expression for shear flow $q = f_s t$ will now be developed for the beam of circular cross-section.

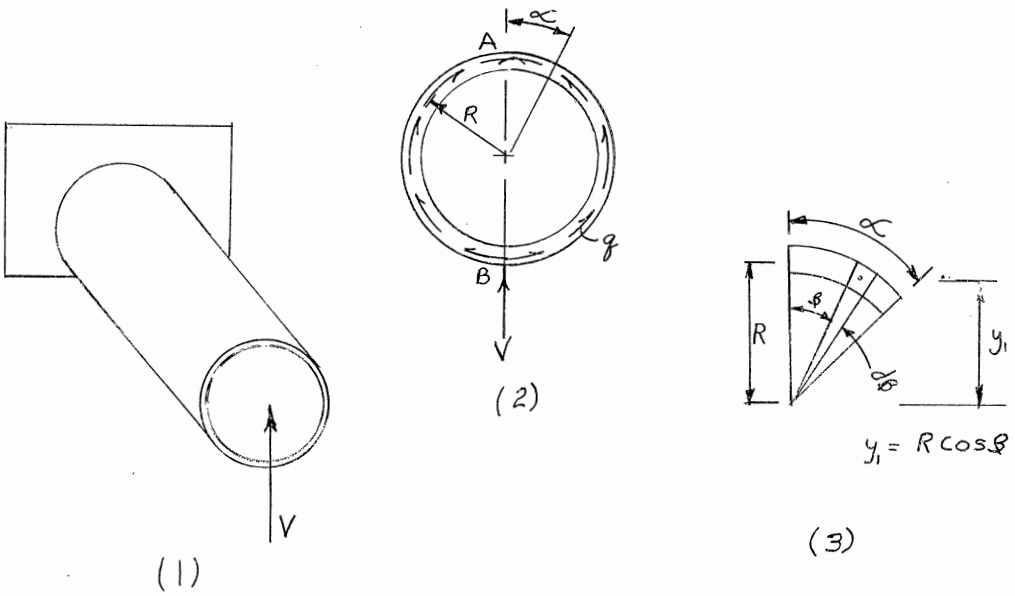

FIGURE 8

An approximate value of the moment of inertia derived from the assumption that the entire area is concentrated at the distance R from the center of the tube will be sufficiently accurate for finding the shear flow or shearing stress.

$$\text{Cross-sectional area} = 2\pi Rt$$

$$\text{Polar moment of inertia} = 2\pi Rt R^2$$

$$= 2\pi R^3 t$$

$$I_X = I_Y = \frac{I_p}{2} = \pi R^3 t$$

The shear flow is zero at the intersection of the centerline with the top and bottom portions of the cross-section (points A and B) due to symmetry. The integral of $f_s = \frac{V}{Ib}\int y\,dA$ represents the moment of the area between the upper center line and the point y_1 as shown in Figure 8 (3), where y_1 is the distance from the neutral axis to the point where the shear flow or shearing stress is desired.

$$\int y\,dA = \int_0^{\alpha} R^2 t \cos\beta\, d\beta$$

$$= R^2 t \sin\alpha$$

$$q = \frac{V}{I}\int y\,dA$$

$$= \frac{V}{\pi R^3 t} R^2 t \sin\alpha$$

$$q = \frac{V}{\pi R}\sin\alpha$$

In airframe analysis, this expression is frequently used for determining the shear flow in a circular fuselage. The longitudinal stiffening members, although they are concentrated areas, usually have approximately a uniform spacing around the circumference. It is often sufficiently accurate to assume these areas distributed along the circumference of the fuselage when determining the shear flow.

The shearing stresses due to bending and due to torsion are collinear quantities, since each is tangent to the cross-section boundary. They may be superimposed to give the following result:

$$f_s = \frac{T}{2\pi R^2 t} \pm \frac{V}{\pi R t} \sin\alpha$$

The $\pm$ sign is used with due respect to the direction of the shearing stresses.

When considering the torsion of thin-walled cylinders, it was assumed that the stressed material acted elastically and did not buckle, and that the wall thickness was comparatively small and did not vary abruptly. These assumptions are also made regarding the present problem. It is reasonable to assume that the shearing stress in thin-walled cylinders due to torsion will be related to the applied torque by a constant, or by a well ordered function, up to a certain point of stress, at which the structure should be expected to assume some of the characteristics of instability. When a cylinder is subjected to torsion, a point of stress may be reached at which the structure buckles, characterized by wrinkling of the walls. In an unstiffened cylinder, immediate collapse takes place. But if the cylinder is stiffened by rings and longitudinal members, it will continue to carry considerably more load by tension field beam action, and if plastic flow of material does not occur in the structure as a whole, it will return to its original shape, possibly with no wrinkles visible to the eye. In fact, the type of thin-walled cylinders which are common in aircraft construction will usually fail ultimately by the instability of one of the stiffening members, and not by the instability of the shell. The point at which ultimate failure takes place in a thin-walled cylinder which is stiffened by rings, frames or

bulkheads, and by longitudinal members is, of course, of concern. It would be difficult to obtain a set of analytical expressions for the stresses in the shell and stiffeners of thin-walled cylinders which were applicable to all designs. Therefore, structural testing has often been depended upon to furnish design information and guidance for engineers. Publications of research and testing programs on this subject dating back twenty-five years and conducted under the auspices of the National Advisory Committee for Aeronautics, Washington, D. C., are readily available. Indications are that earlier U. S. publications and translations of European papers can also be obtained. Most research and testing programs regarding this subject have for their main purpose the examination of the process at ultimate failure, and from the testing of a large number of different structural configurations, to better aid the judgement of the engineer in the design of the product. In the reports of these tests are found formulas for the torque and stresses in the shell and stiffeners at failure. Such formulas may relate the D/t ratio (diameter of the cylinder to the thickness of the shell) and the spacing of stiffeners and bulkheads with the applied torque at failure. Nearly all reports of tests on thin-walled tubes show, by curves and graphs, various functions of the stressed structure with respect to the applied torque. A particularly informative report for a person first studying the subject of thin-walled cylinders under torsion is "Torsion Tests of Aluminum Alloy Stiffened Circular Cylinders," by J. W. Clark and R. L. Moore, NACA TN 2821, available from the National Advisory Committee for Aeronautics, Washington, D. C.

PART VI

TORSIONAL SHEARING STRESSES IN THIN-WALLED ELLIPTICAL CYLINDERS

According to St. Venant's principle for torsion of bars, the torsional stress f_s in a hollow tube is given approximately by the expression

$$f_s = \frac{T}{2At}$$

where T is the torsional moment on the section, A is the area enclosed by the mean perimeter, and t is the wall thickness at any point where the stress is desired. For an elliptical thin-walled tube, $A = \pi bh$ where b is the semi-major axis and h is the semi-minor axis of the mean perimeter of the elliptical cross-section. Therefore

$$f_s = \frac{T}{2\pi bht} \tag{6}$$

Prior to wrinkling of the shell, the conditions of stress within the walls of the cylinder will be given by equation (6) in accordance with the membrane analogy for torsion. After the first wrinkling of the shell has occurred, the stress in the shell probably will vary with the degree of buckling. In the formulation of equation (6), then, the assumptions are made that the cylinder does not assume any inelastic deformation, and that the wall thickness is comparatively small and does not change abruptly.

It has been concluded from torsion tests of a large number of thin aluminum cylinders of elliptical cross-section that the shearing stresses at ultimate torque are the same as those for the circumscribed circular cylinder of the same sheet thickness and length. (Lundquist, 1935).

PART VII

SHEARING STRESSES IN A THIN-WALLED ELLIPTICAL CYLINDER DUE TO BENDING FROM A VERTICAL FORCE

As stated previously, a vertical shearing force parallel to the beam cross-section produces a shearing stress of varying intensity over the cross-section. This shearing stress is given by the following expression, provided no torsion or unsymmetrical bending exists:

$$f_s = \frac{V}{Ib} \int_{y_1}^{c} y dA$$

This formula was previously developed for a general section. In the development of the above formula, the difference in bending moments on two adjacent sections of the structure was used. It may be seen that the ratio of the bending stress to the shearing stress may vary along the span for a given loading and cross-section, and that the ultimate strength of the structure may depend on this ratio. Data from a large number of tests of thin-walled elliptical cylinders under combined transverse shear and bending in the plane of the major axis has been recorded (Lundquist, 1935). It has been concluded that at small values of f_b/f_v (the bending stress at the extreme fibre divided by the beam shearing stress at the neutral axis) failure occurred in shear, and as f_b/f_v approached zero (a condition of pure transverse shear), the shearing stress at a neutral axis at failure, as calculated by the ordinary beam theory, was approximately 1.25 times the shearing stress at failure in torsion. At large values of f_b/f_v, the failure occurred in bending. At

intermediate values of f_b/f_v, there was a transition from shear to bending failure. It can be understood that the efficiency of a thin-walled cylinder, in regards to its load-carrying capacity versus weight, can be raised considerably by the addition of stiffening members, such as frames, rings, and longitudinal members. In view of the purpose of this report, it is considered necessary that an examination be made of the shearing stress or shear flow distribution in a thin-walled stiffened cylinder under the action of a vertical shearing force.

The analysis of a thin-walled unstiffened cylinder under pure torsion has previously been discussed. The addition of longitudinal stiffeners does not affect this analysis other than possibly adding shear area, provided the magnitude of the shearing stresses in the shell is not such as to cause it to buckle. After buckling of the shell, a properly stiffened cylinder will continue to carry load by a series of interesting actions, using the combination of shell and stiffeners to a great advantage. The mechanism is known as "tension field beam action"; it is not discussed in this report but is reserved for future study by the author.

The effect on the shear analysis of the addition of longitudinal stiffeners to a thin-walled cross-section under the action of a load parallel to the cross-section deserves consideration. Figure 9 is a sketch of a portion of a constant cross-section box beam of length d with two longitudinal stiffeners, AB and DE, attached to a thin metal shell. The difference in the axial load in the longitudinal members (called stringers) between the two cross-sections can be found by writing the equation for moments about point B, using arm d with the assumption that the curved shell and web resist no moment.

$$\Delta P = V\frac{d}{h}$$

For future convenience, let d equal 1 inch.

An examination of Figure 9 will disclose that these forces ΔP must be balanced by the shear flows shown (shear flow $q = f_s t$).

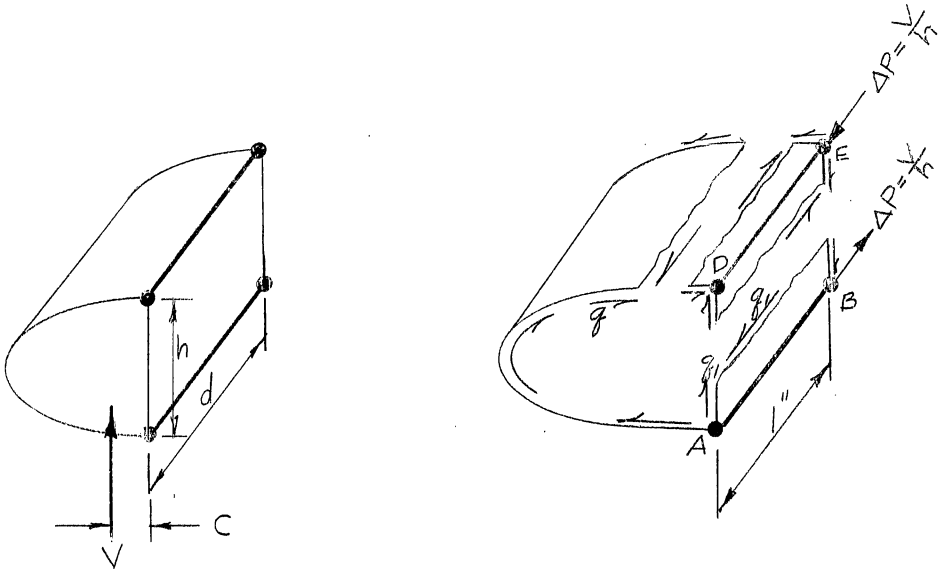

FIGURE 9

By summing forces in the horizontal direction,

$$q_1 = \Delta P - q$$

From the membrane analogy for torsion, previously discussed,

$$q = \frac{T}{2A} = \frac{Vc}{2A}$$

$$q_1 = \frac{V}{h} - \frac{Vc}{2A}$$

q, q_1, h, c and V are noted on the figure and A is the area enclosed by the mean perimeter of the cross-section.

These results may be visualized by replacing the loading situation shown with a vertical force V applied at A and a torsional couple applied

to the cross-section. If the curved portion of the shell and the vertical web ABED resist no moment, the contribution of V to the shear flow q_1 will be $\frac{V}{h}$ and that of the torsional moment will be $\frac{Vc}{2A}$ acting in the opposite direction. The shear flow q in the curved portion of the shell will, of course, be $\frac{Vc}{2A}$.

The shear analysis of a thin-walled box beam incorporating many stringers can be made in a similar manner by taking advantage of the relationship between the differences in load ΔP in each stringer and the shear flows q in the adjacent shell sections. Reference is made to Figure 10.

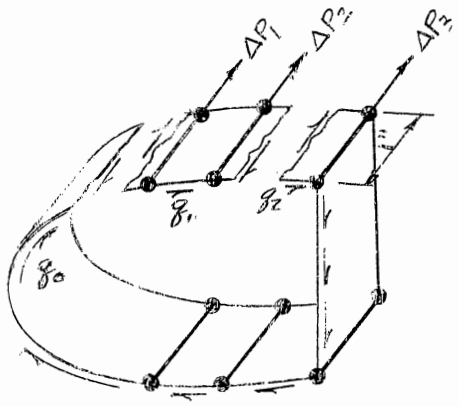

FIGURE 10

From a summation of longitudinal loads on various stringers, the shear flows may all be expressed in terms of one unknown shear flow q_o. This shear flow may then be obtained by equating the moments of the shear flows to the external torsional moment about a longitudinal axis.

With reference to Figure 10, it can be observed that:

$$q_1 = q_o + \Delta P_1$$

$$q_2 = q_0 + \Delta P_1 + \Delta P_2$$

$$q_n = q_0 + \sum_{o}^{n} \Delta P_n$$

where $\sum_{o}^{n} \Delta P_n$ represents the summation of all stringer loads ΔP between the portion of the shell on which q_o acts and any point of desired shear flow. After expressing all the shear flows in terms of the unknown q_o, the value of q_o may be found from torsional moments on the cross-section. Peery (1950) has given an excellent example illustrating the simplicity of this method and affording a visualization of the shearing stress distribution of single cell, multi-stringer thin-walled sections.

It has been noted that all of the previous discussions of the shear analysis of thin-walled cylinders with longitudinal stiffeners is valid provided the shell does not buckle, or undergo any inelastic deformation. Upon buckling of the shell, the structure transfers further load by a degree of tension field beam action. This subject is not discussed in this report.

PART VIII

SHEARING STRESSES IN TAPERED BEAMS

In the preceding discussions of the shear analysis of thin-walled beams, it has been stipulated that the cross-sections of the beam remain constant. Often, all of the material of such a beam can not be fully utilized. For example, the material near the free end of a cantilever beam subjected to bending loads may be lightly stressed, whereas the material near the fixed end may be comparatively highly stressed. Increased efficiency, with regard to strength-weight ratio, can be obtained by designing the beam so as to cause the bending stresses to be nearly constant along its length. Such a design may result in a tapered beam. The wing of an airplane is an example. Although no appreciable error in the bending stresses is introduced by using the flexure formula for the tapered beams usually found in aircraft practice, considerable error may be introduced in the shear stresses of such a beam by using the beam shear formula, $f_s = \frac{V}{Ib} \int ydA$. Another approach must be used for the determination of the shear stresses in tapered beams.

The tapered beam shown in Figure 11 consists of two concentrated flange areas joined by a vertical web which is assumed to resist no bending. The bending loads are assumed to be resisted by axial forces in the flanges. The flanges are straight and are inclined at angles u_1 and u_2 to the horizontal. The resultant axial load in the flanges must be in the direction of the flanges and must have horizontal components $P = V \frac{b}{h}$.

The vertical components of the loads in the flanges P tan u_1 and P tan u_2 which are shown in Figure 11 (2) resist some of the external shear V.

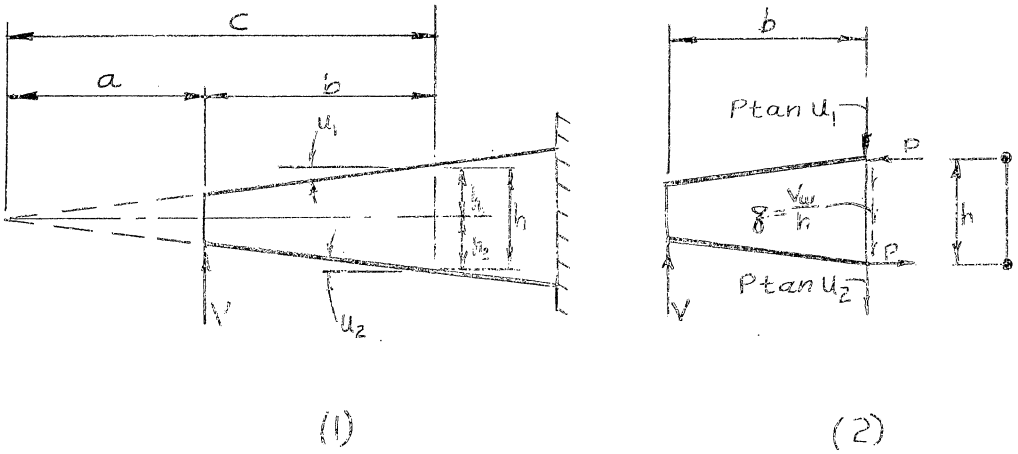

(1) (2)

FIGURE 11

Designating this shearing force resisted by the flanges as V_f and that resisted by the webs as V_w, the following equations apply:

$$V = V_f + V_w$$

$$V_f = P(\tan u_1 + \tan u_2)$$

$$\tan u_1 = \frac{h_1}{c} \; ; \; \tan u_2 = \frac{h_2}{c}$$

$$\tan u_1 + \tan u_2 = \frac{h+h_2}{c} = \frac{h}{c}$$

Substitute the last expression in the above equation for V_f.

$$V_f = P\frac{h}{c} \qquad (7)$$

Equation (7) will apply for a beam with any system of vertical loads.

Since $P = V\frac{b}{h}$; $V_f = V\frac{b}{c}$. (8)

From the geometry of Figure 11,

$$V_w = V - V_f$$

$$= V\left(1 - \frac{b}{c}\right)$$

$$V_w = V\frac{a}{c} \tag{9}$$

Equations (8) and (9) may be expressed in terms of h_o and h by making use of the proportion $\frac{a}{c} = \frac{h_o}{h}$

$$V_w = V\frac{h_o}{h} \tag{10}$$

$$V_f = V\frac{h - h_o}{h} \tag{11}$$

If a tapered beam has two equal flanges of area A and a depth between flanges of h, the beam shear formula may be used to obtain the shear flow by substituting V_w for V as follows,

$$q = \frac{V_w}{I}\int y\,dA$$

$$= \frac{V_w}{2A\left(\frac{h}{2}\right)^2}\left(A\frac{h}{2}\right)$$

$$q = \frac{V_w}{h}$$

A similar method may be used to find the shear flow in a tapered beam with several flange areas, if the areas of the flanges remain constant along the span. The following example will demonstrate a method of computing stringer loads and shear flow for a tapered box beam with several flanges whose area remains constant along the span.

It is desired to find the stringer loads and shear flows for the tapered box beam shown in Figure 12.

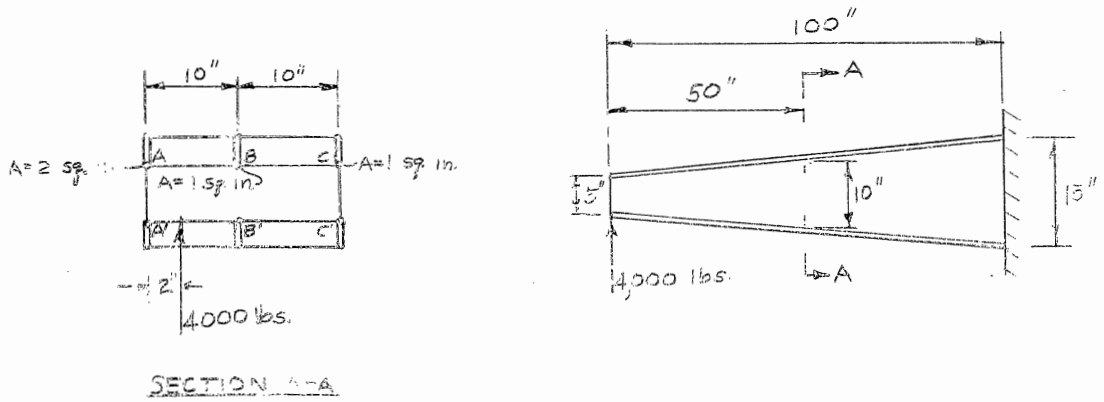

FIGURE 12

Area of stringers	Angle Functions
$A_A = A_{A'} = 2$ sq. in.	$\tan u_1 = .05$
$A_B = A_{B'} = A_C = A_{C'} = 1$ sq. in.	$\tan u_2 = .05$

At section A-A.

$$h = 10 \text{ in.}$$

$$I = 2(2 + 1 + 1)5^2 = 200 \text{ (in.)}^4$$

It is assumed that the moment of inertia of the stringer areas about their own bending axis is negligible.

$$f_b = \frac{MV}{I} = \frac{200{,}000 \times 5}{200} = 5{,}000 \text{ lbs./in.}^2$$

P_{A_H} = Horizontal component of load in stringer A and A'.

$$P_{A_H} = 5000 \times 2 = 10{,}000 \text{ lbs.}$$

$$P_{B_H} = P_{C_H} = 5000 \times 1 = 5000 \text{ lbs.}$$

P_{A_V} = Vertical component of load in stringers A and A'.

$$P_{A_V} = P_{A_H} \tan u_1$$

$$= 10{,}000 \times .05 = 500 \text{ lbs.}$$

$$P_{B_V} = P_{C_V} = 5000 \times .05 = 250 \text{ lbs.}$$

V_f = Vertical shearing load resisted by all flanges

$$V_f = 2 P_{A_V} + 2 P_{B_V} + 2P_{C_V}$$

$$= 1000 + 500 + 500$$

$$= 2000 \text{ lbs.}$$

V_w = Vertical shearing load resisted by both webs, A-A' and C-C'.

$$V_w = 4000 - 2000$$

$$= 2000 \text{ lbs.}$$

These loads are shown in the following sketch.

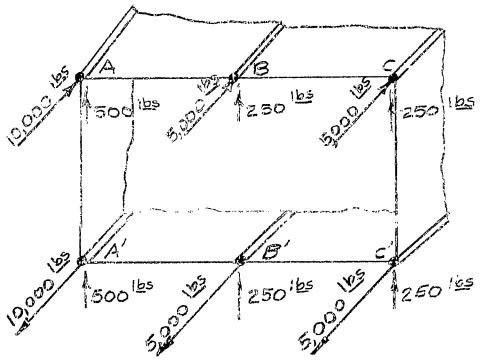

FIGURE 13

To obtain the shear flows in the webs, it is convenient to consider a portion of the beam between parallel cross-sections 1 inch apart, as discussed in Part VI, and illustrated by Figure 14.

The change in bending stress on a stringer between two cross-sections one inch apart is

$$\Delta f_b = \frac{V_w y}{I}$$

$$= \frac{2,000 \times 5}{200}$$

$$= 50 \text{ lbs per sq. in.}$$

The change in axial load on a stringer of area A_f is considered to be:

$$\Delta P = \frac{V_w y}{I} A_f \qquad (12)$$

$$\Delta P_A = 50 \times 2 = 100 \text{ lbs.}$$

$$\Delta P_B = \Delta P_C = 50 \times 1 = 50 \text{ lbs.}$$

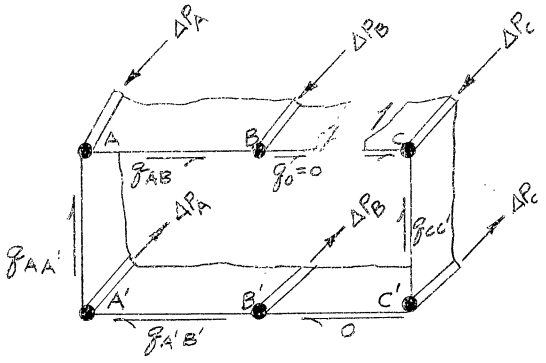

FIGURE 14

The error involved in the use of equation (12) is considered negligible for the usual tapered beams found in aircraft practice. The true value of the axial load in a stringer is $\frac{\Delta P}{\cos u}$.

If the assumption is made that the web BC is cut, $q_o = 0$, and the relative shear flows $q_{AA'}$, q_{AB}, and $q_{CC'}$ can be determined by the procedure discussed in PART VII of this report. The relative shear flows are:

$q_{AA'}$ = 150 lbs. per in.

q_{AB} = 50 lbs. per in.

$q_{CC'}$ = -50 lbs. per in.

$q_{C'B}$ = 0 lbs. per in.

$q_{B'A'}$ = 50 lbs. per in.

The minus sign denotes a counter-clockwise shear flow.

The shear flow q_o must now be found and the relative values $q_{AA'}$, q_{AB}, $q_{C'B'}$, and $q_{CC'}$ corrected. q_o may be found by taking moments about any spanwise axis, such as one through point O, Figure 15 (1).

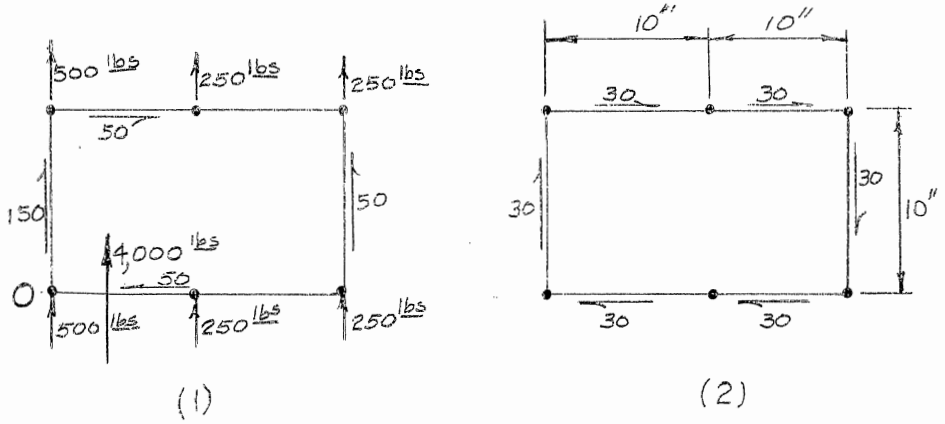

FIGURE 15

The sum of moments of external forces plus the sum of moments of internal forces equal zero.

$$-(4000 \times 2) - (2 \times 250 \times 10) - (2 \times 250 \times 20) - (50 \times 10 \times 20)$$
$$+ (50 \times 10 \times 10) + \left[(20 \times 10) + (10 \times 20)\right] q_o = 0$$

q_o = 30 lbs. per in. in a clockwise direction as shown in Figure 15 (2).

The resultant shear flows are as follows:

$q_{AA'} = 150 + 30 = 180$ lbs. per in.

$q_{AB} = 50 + 30 = 80$ lbs. per in.

$q_{BC} = q_o = 30$ lbs. per in.

$q_{CC'} = -50 + 30 = -20$ lbs. per in.

$q_{C'B'} = q_o = 30$ lbs. per in.

$q_{B'A'} = 50 + 30 = 80$ lbs. per in.

The resultant shear flows and stringer shear loads are shown in Figure 16.

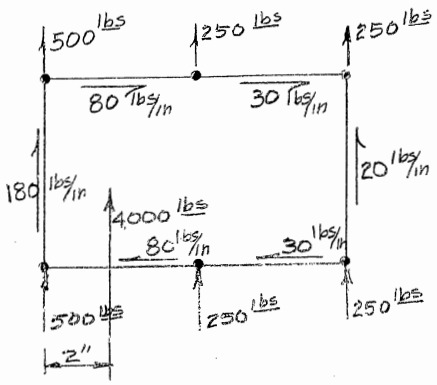

FIGURE 16

Tne analysis of this type of structure is especially suited to a tabular form. Before proceding with the solution of this problem utilizing a tabular form, a few remarks regarding aircraft practice in the stress analysis of wings may be in order. An airplane wing usually has many stringers, and is tapered in both depth and width. Each stringer may have a different angle with both the horizontal and vertical. A solution for both the horizontal and vertical components of all stringer loads would usually require more work than would be justified. An approximate method of obtaining the torsional moment of the horizontal and vertical components of the stringer forces is usually sufficiently accurate. One approximate method consists of taking torsional moments about some point in the cross-section about which the stringer forces produce no appreciable torsional moment and of omitting the stringer forces in the moment equation. A torsional axis joining the centroids of the cross-section may be satisfactory.

In the foregoing problem, the resultant of the vertical forces in

the stringers is 7.5 inches from the left web, or through the centroid of the areas. Point 0' shown in Figure 17 will be used as the center of moments. The torsional moment of the external shear about 0' is then 4,000 x 5.5 = 22,000 inch-pounds. Since the vertical components of the stringer forces are neglected, only the shearing forces carried by the webs will be assumed acting. From equation (10)

$$V_w = V\frac{h_o}{h} \qquad \Delta P = \frac{V_w\, y}{I} A_f$$

$$= 4{,}000\ \frac{5}{10} \qquad = \frac{2000}{200} 5A_f$$

$$V_w = 2{,}000 \text{ lbs} \qquad = 50 A_f$$

where A_f is the area of the flange. These values of ΔP are tabulated in column (2) of Table I. The negative sign indicates compression. The relative shear flows, q_{AB}, etc., denoted as q' and shown in column (3) are obtained by a summation of ΔP in column (2). The terms in column (4) represent twice the areas enclosed by the corresponding webs and the lines joining the extremeties of the webs and the center of moments, as shown in Figure 17. The moments of the shear flows in the webs are obtained in columns (5) as the product of the terms in columns (3) and (4). The total moment of the shear flows q' is 10,000 inch-pounds and is obtained as the sum of the terms in column (4). The sum of the moments of the external forces plus the sum of the moments of the internal forces equals zero.

$$22{,}000 - 10{,}000 - 400\ q_o = 0$$

$$q_o = 30 \text{ lbs. per in.}$$

The final shear flows are tabulated in column (6) and are the result of algebraic addition of q_o and q'.

TABLE I

AN EXAMPLE OF A TABULAR FORM FOR SHEAR FLOW ANALYSIS COMPUTATIONS

FLANGE (1)	ΔP (2)	$q' = \Sigma \Delta P$ (3)	2 A (4)	2A q' (5)	$q = q_o + q'$ (6)
C	-50	-50	125	-6,250	-20
C'	+50	0	50	0	30
B'	+50	+50	50	2,500	80
A'	+100	+150	75	11,250	180
A	-100	+50	50	2,500	80
B	-100	0	50	0	30
			400	10,000	

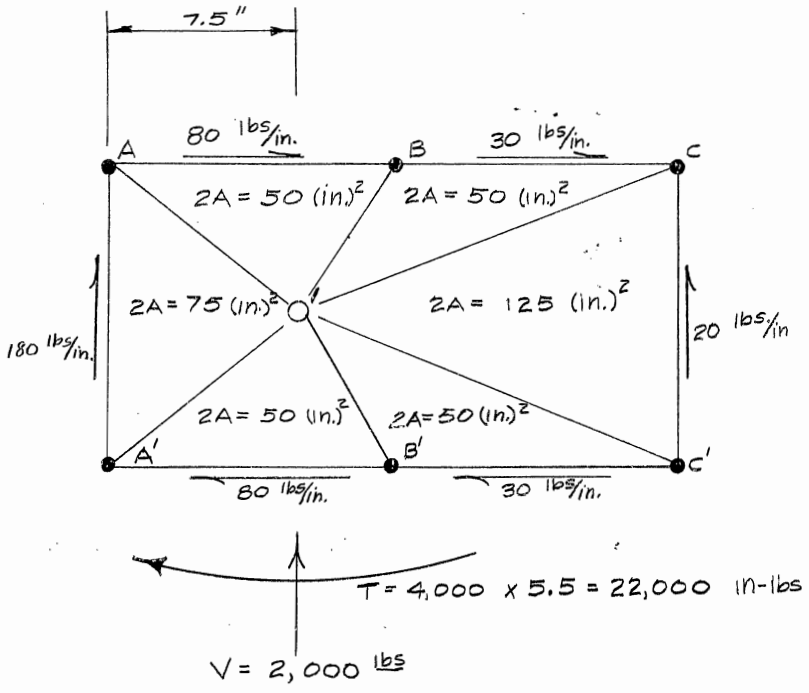

FIGURE 17

PART IX

AN EXAMPLE PROBLEM OF A THIN-WALLED MULTI-CELL STRUCTURE

PART I through PART VIII of this report have been concerned with single cell structures. The shear analysis of multi-cell structures can follow the same methods as those used for the single cell. The assumptions used in the formulation of equations for the shear flow determination of the single cell will apply to multi-cell structures. When concerned with the torsional deformation of multi-cell structures, the additional assumption is made that the transverse stiffeners are sufficiently rigid so that all cells rotate through the same angle. Transverse stiffening members may be called bulkheads if they are solid, or almost so, or they may be called frames if they are the open, ring type.

The multi-cell structure shown in Figure 18 is a cantilever beam of three cells stiffened in a transverse direction by equally spaced bulkheads which are assumed to be rigid and to remain undistorted under load. These bulkheads act as the loading points for point loads of 1,000 pounds each applied in a single line in the plane of one of the webs as shown in Figure 19. The sheet metal shell and longitudinal "T" and angle stiffeners are of the same material. Cell 1 is enclosed by a semi-elliptical section, cell 2 by a rectangular section and cell 3 by a semi-circular section. It is required to find the shear flow at section A-A of the three cell structure shown in Figure 18.

Preliminary data

Section properties

"T" section: 1 1/4 x 1 1/2 x 1/8

$I_{NA} = 0.3\ (in.)^4$ Area = $.37\ (in.)^2$

Angle section: 2 1/2 x 2 1/2 x 1/8

$I_{NA} = .37\ (in.)^5$ Area = $.62\ (in.)^2$

Moment of inertia of the cross-section:

Assume that the shell and webs resist no bending stress.

Neglect the moment of inertia of the "T" and angle sections about their own bending axis.

$I = 2 \times (18)^2 \times$ Area of "T" + $4 \times (18)^2 \times$ Area of angle

$= 1040\ (in.)^4$

Area enclosed by the periphery of cell 1, cell 2, and cell 3

$A_1 = 1/2\ \pi \times 30 \times 18$
$= 850\ (in.)^2$

$A_2 = 80 \times 36$
$= 2880\ (in.)^2$

$A_3 = 1/2\ \pi\ (18)^2$
$= 510\ (in.)^2$

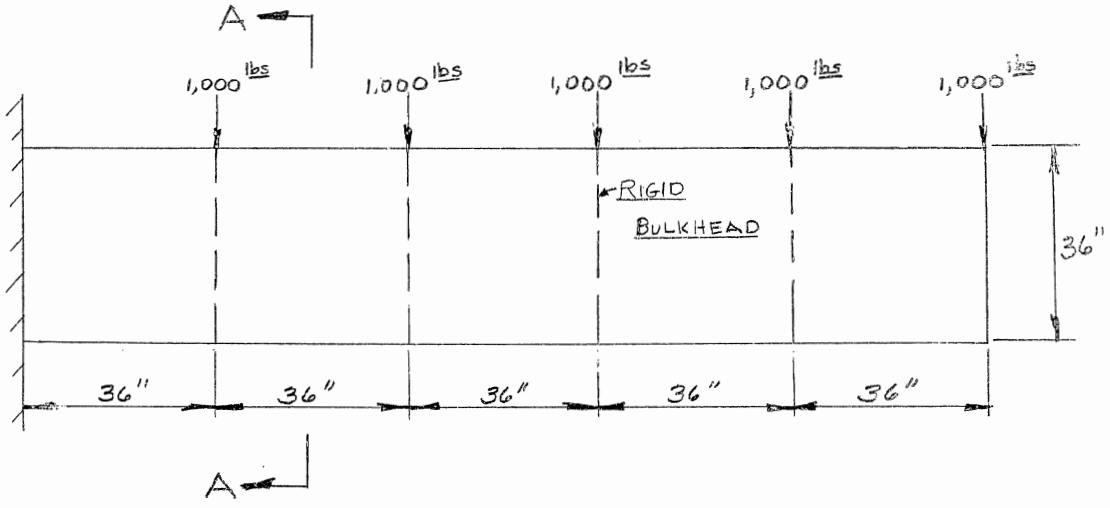

FIGURE 18

Lengths of curved portions of the cross-section:

Length A'FA = 1/2 x 4 x 30 x 1.395

= 83.75 in.

Length CGC' = 18π

= 56.6 in.

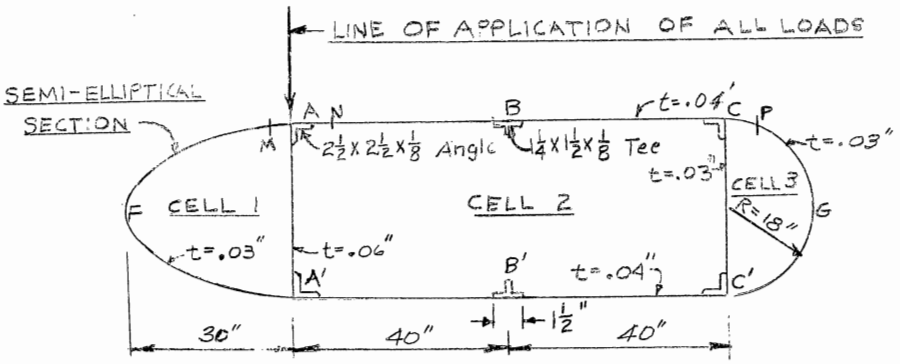

SECTION A-A

FIGURE 19

Shear flows q' from bending only are computed as follows:

It is assumed that:

1. The shear flows at points M, N, and P are equal to zero.

2. The shell and webs resist no bending moment.

3. The introduction of any torsion will not affect the axial load in the stringers.

$$\Delta M = M_2 - M_3 = 4000 \times 36$$
$$= 144,000$$

$$f_{b_2} - f_{b_3} = \frac{\Delta M\, y}{I}$$
$$= \frac{144,000 \times 18}{1040}$$
$$= 2500 \text{ in-lbs}$$

$$\Delta P_A = 2500 \times .62 = 1550 \text{ lbs.}$$

$$\Delta P_C = 2500 \times .37 = 925 \text{ lbs.}$$

REFERENCE IS MADE TO FIGURE 20.

$q'_{A'FA} = 0$

$q'_{AB} = 0$

$q'_{AA'} = +\frac{1550}{36} = +43 \text{ lbs/in.}$

$q'_{Bc} = -\frac{925}{36} = -25.7 \text{ lbs/in.}$

$q'_{cBc'} = 0$

$q'_{cc'} = -\frac{925+1550}{36} = -68.5 \text{ lbs/in.}$

$q'_{Bc'} = -\frac{925}{36} = -25.7 \text{ lbs/in.}$

$q'_{A'B'} = 0$

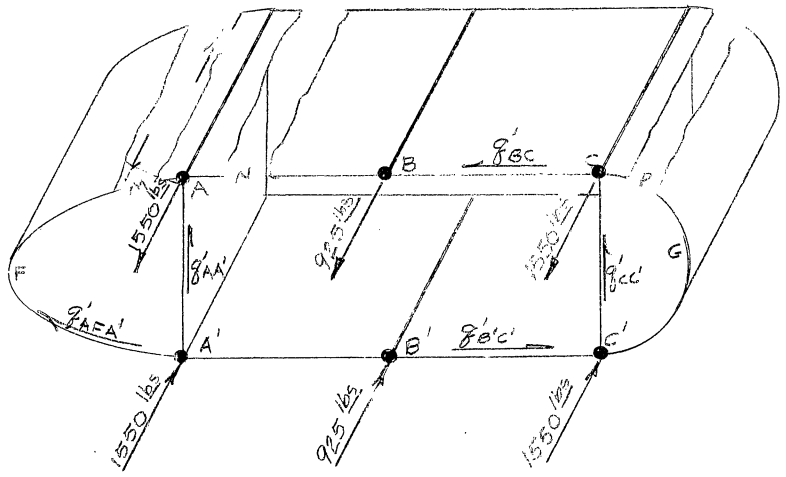

FIGURE 20

Since the shear flows at points M, N, and P were assumed equal to zero, the shear flows computed above are relative ones and must be corrected. Regardless of the existence of torsion on the cross-section, the moments of the internal shear flows plus the moments of the external forces about any point would be equal to zero. If the external loads cause no torsion on the cross-section, the angles of twist in each

cell would also be zero. The values of three constant shear flows - one in each cell - could then be determined and added algebraically to the shear flows q' from bending to arrive at the true shear flows in the cross-section.

Since the cross-section of the structure considered here does have a torsional moment applied to it, there will be a twist, or torsional deformation, of each cell. If the assumption is made that the angles of twist in the three cells are equal, a constant shear flow for each cell can be found which is compatible with this assumption. This unknown shear flow for each cell will be composed of the shear flow from torsion alone and the correction to the shear flow from bending.

Introduction of the shear flows from torsion and correction to the shear flows from bending follow.

It is assumed that:

1. The angles of twist for each cell θ_1, θ_2, and θ_3, are equal.
2. The shell and web material act elastically and do not buckle.
3. The modulus of rigidity, G, is constant for the material of the structure.

Since the following analysis makes use of the equation for the angular deformation θ, it is desirable to discuss its derivation.

Much of the classical theory of statically indeterminate structures has been developed for the analysis of comparatively heavy structures in which shearing deformations are of minor importance and can usually be neglected. In the analysis of thin metal shell structures, the shear stress distribution is usually of major importance. The deflections caused by shearing deformations may be determined by energy methods, such as that

of virtual work, in the same manner that other types of deflections are found. Perhaps one of the more simple approaches would be to consider the shearing deformation of a rectangular plate of thickness t, width a, and length b as shown in Figure 21. The shearing strain is obtained from the relation

$$\gamma = \frac{f_s}{G} = \frac{q}{tG} \tag{13}$$

where f_s is the shearing stress and q is the shear flow $f_s t$. The strain energy of shearing deformation is

$$U = \frac{f_s t a b}{2} \gamma$$

$$= \frac{q}{2} a b \frac{q}{tG}$$

$$U = \frac{q^2}{2tG} ab \tag{14}$$

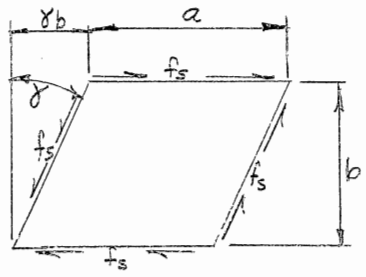

FIGURE 21

A unit virtual load applied at the point of desired deflection δ produces a system of shear flows q_u in the webs. The force $(q_u a)$ acts through the displacement γb. By the principle of conservation of energy, the external work must be equal to the internal work accomplished on the structure.

$$(1)\delta = \sum q_u \gamma a b$$

$$= \sum \frac{q_u q a b}{tG} \tag{15}$$

The summation symbol is used to include all webs of the structure which affect the deflection. It may be noted that q_u represents the shear flows due to the virtual load and q represents the actual shear flows which produce the deformation of the structure. Equation (15) applies only to elastic deformations which satisfy equation (13).

By reference to Figure 22, an expression can be obtained for the angular deformation of the box beam by applying a unit virtual couple T. The resulting virtual flows are $q_u = \frac{1}{2A}$ where A is the area enclosed by the shell. If the webs have dimensions a = Δs and b = L, the angle of twist may be found by substituting these values into equation (15) to obtain

$$\theta = \sum \frac{q\, ak}{2AtG}$$

$$\theta = \sum \frac{q\, L}{2AtG} \Delta s \qquad (16)$$

where the summation includes all webs of the structure.

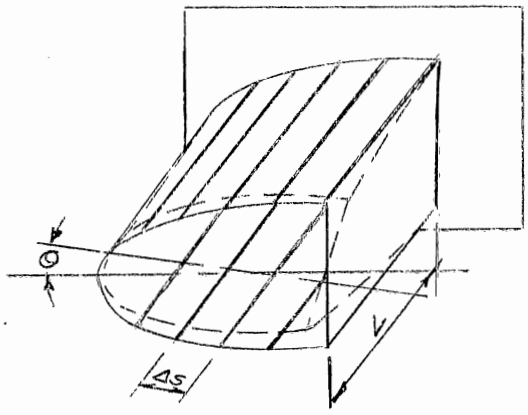

FIGURE 22

Equation (16) may be used for the angular deformation of a multi-cell

structure, if the summation is evaluated around any closed path and the area A is enclosed by this path. Thus, for a three cell structure, the summation may be evaluated around the perimeter of any one cell, or of two cells, or around the perimeter of the three cells. The procedure is sometimes defined as a line integral as follows:

$$\theta = \oint \frac{q L}{2 A t G} ds \qquad (16a)$$

where the integral represents an evaluation along a closed path, returning to the starting point. This expression is used in the present problem, considering the values of the summation positive in the clockwise direction. As used in this part of the problem, q is the shear flow which must be added to the relative flexural shear flows, q', to make the angular deformation of each cell the same; L is the length of the member between cross-sections considered, and is equal to 36 in. for all cells; A is the area enclosed by the periphery of a cell; t is the thickness of the walls of the cell; G is the modulus of rigidity of the shell, web, and stiffener materials; and ds is an elemental distance along a cell periphery. The integral is to be evaluated around a cell periphery. θ is the total angle of twist of a cell.

Let θ_1, θ_2, and θ_3 be the angles of twist for cells 1, 2, and 3, respectively.

$$\theta_1 = \frac{L}{2GA_1}\int_1 \frac{q}{t} ds \qquad \theta_2 = \frac{L}{2GA_2}\int_2 \frac{q}{t} ds \qquad \theta_3 = \frac{L}{2GA_3}\int_3 \frac{q}{t} ds$$

Since $\frac{L}{2G}$ is constant, a simplification of computations will be obtained if this quantity is incorporated into the symbol for angle of twist for each cell. The integral $\int_1 \frac{q}{t} ds$ for cell 1 can be thought of as being composed of two parts: an evaluation around the path A'FA and an evaluation along AA' as follows:

$$\text{LET } \theta_1' = \frac{\theta_1}{\frac{L}{2G}}$$

$$\int_1 \frac{q}{t} ds = \int_{A'FA} \frac{q}{t} ds + \int_{AA'} \frac{q}{t} ds$$

$$= \frac{q_{A'FA}}{t_{A'FA}} \int_{A'FA} ds + \frac{q_{AA'}}{t_{AA'}} \int_{AA'} ds$$

$q_{AA'}$ is the resultant of the superposition of the shear flow in cell 1 and that in cell 2. Let q_1 designate the shear flow in cell 1 and q_2 the shear flow in cell 2.

Then: $q_{AA'} = q_1 - q_2$ and for cell 1,

$$\int \frac{q}{t} ds = \frac{q_1}{t_{A'FA}} \int_{A'FA} ds + \frac{q_1 - q_2}{t_{A'A}} \int_{A'A} ds$$

These expressions are substituted into the equation for θ_1' and the effect on θ_1' of the flexural shear flows added.

$$\theta_1' = \frac{1}{850}\left[\frac{q_1}{.03}\ 83.73 + \frac{q_1 - q_2}{.06}\ 36\right] - \frac{1}{850}\ \frac{43}{.06}\ 36$$

$$\theta_1' = 3.99\, q_1 - .71 q_2 - 30.4$$

$$\theta_2' = \frac{1}{A_2}\left[\frac{q_2}{t_{AC}}\int_{AC} ds + \frac{q_2 - q_3}{t_{CC'}}\int_{CC'} ds + \frac{q_2}{t_{C'A'}}\int_{C'A'} ds + \frac{q_2 - q_1}{t_{A'A}}\int_{A'A} ds\right]$$

$$+ \frac{1}{A_2}\left[\frac{q'_{BC}}{t_{BC}}\int_{BC} ds + \frac{q'_{CC'}}{t_{CC'}}\int_{CC'} ds + \frac{q'_{B'C'}}{t_{B'C'}}\int_{B'C'} ds + \frac{q'_{AA'}}{t_{AA'}}\int_{AA'} ds\right]$$

$$= \frac{1}{2880}\left[\frac{q_2}{.04}\ 80.0 + \frac{q_2 - q_3}{.03}\ 36 + \frac{q_2}{.04}\ 80.0 + \frac{q_2 - q_1}{.06}\ 36\right]$$

$$+ \frac{1}{2880}\left[\frac{q_2}{.04}\ 80.0 + \frac{q_2 - q_3}{.03}\ 36 + \frac{q_2}{.04}\ 80.0 + \frac{q_2 - q_1}{.06}\ 36\right]$$

$$\theta_2' = -.208\, q_1 + 2.015\, q_2 - .417\, q_3 - 37.49$$

$$\Theta_3' = \frac{1}{A_3}\left[\frac{q_3}{t_{CGC'}}\int_{CGC'} ds + \frac{q_3 - q_2}{t_{CC'}}\int_{CC'} ds\right] + \frac{1}{A_3}\left[\frac{q'_{C'C}}{t_{C'C}}\int_{C'C} ds\right]$$

$$= \frac{1}{5.3}\left[\frac{q_3}{.03}\,56.6 + \frac{q_3 - q_2}{.03}\,36\right] + \frac{1}{5.10}\,\frac{68.5}{.03}\,36\Big]$$

$$\Theta_3' = -2.38\,q_2 + 6.08\,q_3 + 161$$

Then:

$$\Theta_1' = 3.99\,q_1 - .71\,q_2 - 30.4 \qquad (a)$$

$$\Theta_2' = -.208\,q_1 + 2.015\,q_2 - .417\,q_3 - 37.49 \qquad (b)$$

$$\Theta_3' = -2.38\,q_2 + 6.08\,q_3 + 161 \qquad (c)$$

The summation of the torsional moments of the internal shear flows and external loads must be equal to zero for equilibrium. Torsional moments will be computed with respect to stringer A. The external loads will then have a moment of zero with respect to this point. To aid in the visualization of this procedure, Figure 23 is shown with the relative flexural shear flows and q_1, q_2, and q_3 shown thereon.

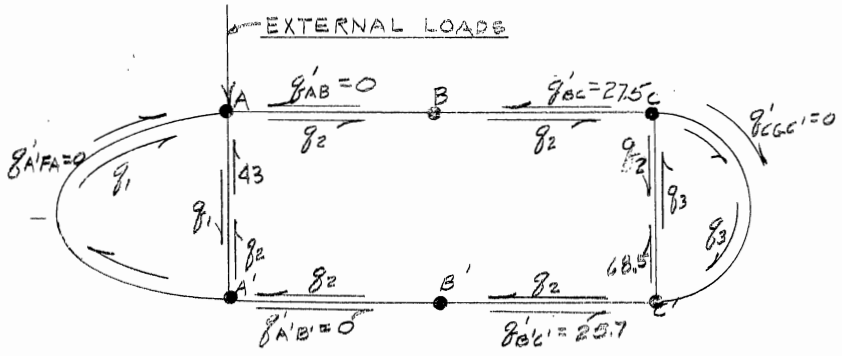

FIGURE 23

$$\Sigma M_A = 0$$

$$+(80 \times 36)(q_2 - 68.5 - q_3) + (80 + \tfrac{2A_3}{36})\,36 q_3 + (36 \times 40)(q_2 - 25.7)$$

$$+(\tfrac{2A_1}{36}\,36 q_1) + (36 \times 40\, q_2)$$

$$1700\, q_1 + 5760\, q_2 + 1020\, q_3 - 234{,}200 = 0 \qquad (d)$$

The simultaneous solution of (a), (b), (c), and (d) yields:

q_1 = +20.7 lbs./in. q_2 = +34.5 lbs./in. q_3 = -.08 lbs./in.

The superposition of q_1, q_2, and q_3 on the relative flexural shear flows, q', yields the required shear flows at the section under consideration. The result is shown in Figure 24.

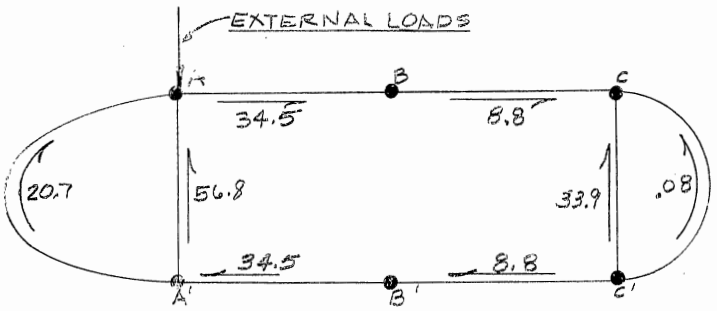

FIGURE 24

The final shear flows, shown in Figure 24, can be checked by use of the three equations of equilibrium, i.e., $\Sigma F_H = 0$, $\Sigma F_V = 0$, and $\Sigma M = 0$.

PART X

AN EXAMPLE PROBLEM ILLUSTRATING A PROCEDURE FOR THE SHEAR ANALYSIS OF AN AIRPLANE WING

The following problem is included in this report to illustrate one method of determining the shearing stresses or shear flows in a thin-walled multi-cell structure of complicated shape subjected to bending and torsional loads. The structure selected is the wing of an actual airplane. It is desired to find the shear flows at station X_{RS} 237 of the wing shown in Figure 25. The method of shear analysis used has been adapted from those methods described by Peery (1950) and Bruhn (1949).

By reference to Figure 25, it can be seen that the wing section is a three-cell "torque box" which is redundant to the second degree. Since the shear flows in the three cells must be determined, three equations relating the shear flows must be found. Following the method of Peery (1950) and Bruhn (1949) and others, the assumption is made that the wing ribs have sufficient rigidity so that the three cells rotate through the same angle under torsional loads. Three equations in four unknowns may then be written containing the three unknown shear flows for the three cells. The fourth equation necessary for a solution may be written as the sum of the external torsional moments plus the sum of the internal torsional moment set equal to zero.

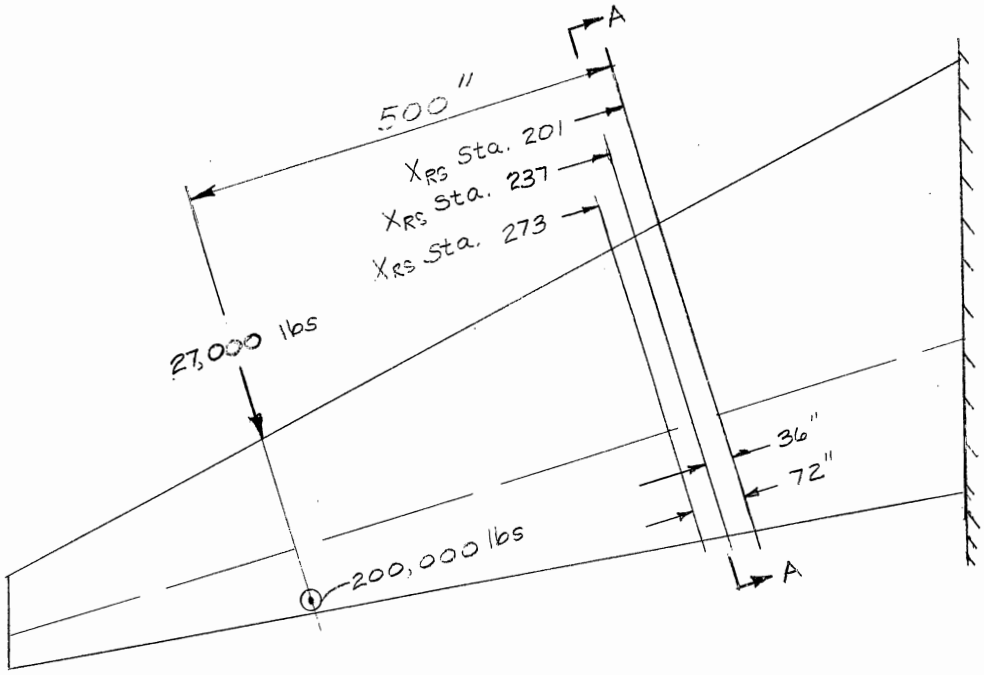

PLAN VIEW

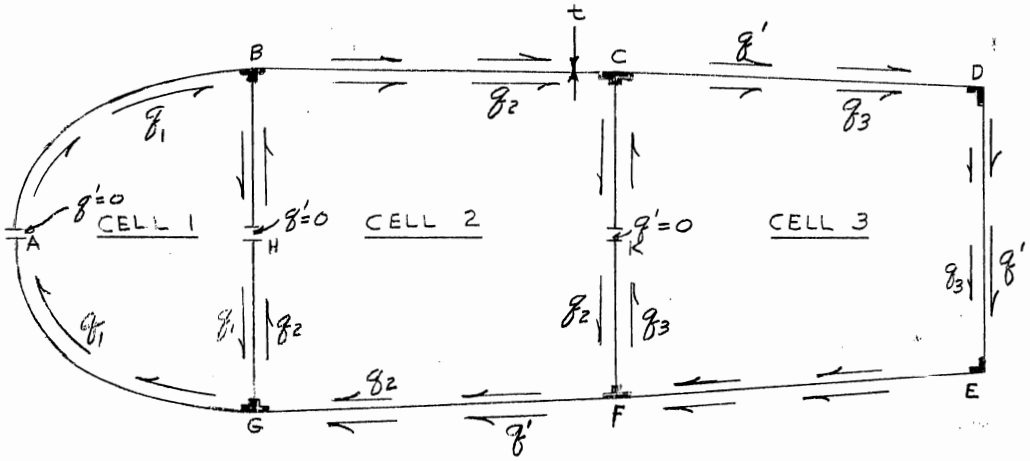

SECTION A-A

AIRPLANE LEFT WING

FIGURE 25

The method of solution of the problem will be illustrated by first writing the three equations for the unknown shear flows in the three cells. Reference is made to Figure 25 for structure geometry and to PART IX for theory and assumptions governing the use of the angular deformation equations:

$$\theta_1 = \sum_1 \frac{q_1 L}{2A_1 t_1 G} \Delta S$$ This equation may be written as:

$$\theta_1 = \frac{q_1 L}{2A_1 G} \sum_1 \frac{\Delta S}{t} \qquad (17)$$

where the subscript 1 refers to the first cell, q_1 is the shear flow, A_1 is the area enclosed by the perimeter of the first cell, G is the modulus of rigidity of the shell material, t is the thickness of the shell, ΔS is the distance along the shell periphery between stringers, and L is the length of the structure between two cross-sections. For convenience, use the symbol ℓ to replace ΔS, and since only relative magnitudes of θ_1, θ_2 and θ_3 need be considered, let L equal 1 unit of linear measurement. Equation (17) then becomes:

$$\theta_1 = \frac{q_1}{2A_1 G} \sum_1 \left(\frac{\ell}{t}\right)$$

In like manner,

$$\theta_2 = \frac{q_2}{2A_2 G} \sum_2 \left(\frac{\ell}{t}\right)$$

and

$$\theta_3 = \frac{q_3}{2A_3 G} \sum_3 \left(\frac{\ell}{t}\right)$$

q_1, q_2, and q_3 in the above equations are the constant shear flows for each cell which must be added to the relative flexural shear flows, q', (to be determined later) in order to make the angular deformations of each cell equal.

In Figure 25, it will be noticed that the webs of the structure are assumed cut at points A, H, and K in accordance with the procedure for determining the shear flows in a closed thin-walled structure. The rel-

ative flexural shear flows q' from wing bending will not appear in the webs assumed to be cut. The shear flows q_1, q_2, and q_3 will appear in all structure webs of their respective cells. In dealing with a wing or other thin-walled, multi-stringer structure, the word "web" may be used to denote the metal shell between any two stringers.

The equations for θ_1, θ_2, and θ_3 may be written

$$2A_1 G\theta_1 = q_1 \sum_1 \left(\frac{l}{t}\right) - q_2 \left(\frac{l}{t}\right)_{GB} \tag{18}$$

$$2A_2 G\theta_2 = \sum_2 q' \left(\frac{l}{t}\right) + q_2 \sum_2 \left(\frac{l}{t}\right) - q_1 \left(\frac{l}{t}\right)_{GB} - q_3 \left(\frac{l}{t}\right)_{FC} \tag{19}$$

$$2A_3 G\theta_3 = \sum_3 q' \left(\frac{l}{t}\right) + q_3 \sum_3 \left(\frac{l}{t}\right) - q_2 \left(\frac{l}{t}\right)_{FC} \tag{20}$$

Assume that G is constant for the material in all cells. Equating (18) and (19) results in the following

$$\frac{q'}{A_1} \sum_1 \left(\frac{l}{t}\right) - \frac{q_2}{A_2} \left(\frac{l}{t}\right)_{GB} + \frac{q_1}{A_2} \left(\frac{l}{t}\right)_{GB} - \frac{q_2}{A_2} \sum_2 \left(\frac{l}{t}\right) + \frac{q_3}{A_2} \left(\frac{l}{t}\right)_{FC} = \frac{1}{A_2} \sum_2 q' \left(\frac{l}{t}\right) \tag{21}$$

Equating (18) and (20) results in the following:

$$\frac{q'}{A_1} \sum_1 \left(\frac{l}{t}\right) - \frac{q_2}{A_1} \left(\frac{l}{t}\right)_{GB} + \frac{q_2}{A_3} \left(\frac{l}{t}\right)_{FC} - \frac{q_3}{A_3} \sum_3 \left(\frac{l}{t}\right) = \frac{1}{A_3} \sum_3 q' \left(\frac{l}{t}\right) \tag{22}$$

A third equation is obtained by the summation of torsional moments on the section.

$$T_{EXT} + \sum_2 2Aq' + \sum_3 2Aq' + 2A_1 q_1 + 2A_2 q_2 + 2A_3 q_3 = 0$$

where T_{EXT} is the torsional moment on the section due to external loads. A simplification of the above equation will result by letting twice the areas applicable to the computations of q' be designated by the symbol m. This facilitates tabular computations involving the shear flow q' from wing bending. The equation then becomes

$$T_{EXT} + \Sigma mq' + 2A_1 q_1 + 2A_2 q_2 + 2A_3 q_3 = 0 \qquad (23)$$

By rearranging and combining terms in equations (21), (22) and (23), a more suitable form is obtained.

$$\left[\frac{1}{A_1}\sum_1\left(\frac{l}{t}\right) + \frac{1}{A_2}\left(\frac{l}{t}\right)_{GB}\right] q_1 - \left[\frac{1}{A_2}\sum_2\left(\frac{l}{t}\right) + \frac{1}{A_1}\left(\frac{l}{t}\right)_{GB}\right] q_2 + \left[\frac{1}{A_2}\left(\frac{l}{t}\right)_{FC}\right] q_3 = \frac{1}{A_2}\sum_2 q'\left(\frac{l}{t}\right) \qquad (21a)$$

$$\left[\frac{1}{A_1}\sum_1\left(\frac{l}{t}\right)\right] q_1 - \left[\frac{1}{A_1}\left(\frac{l}{t}\right)_{GB} - \frac{1}{A_3}\left(\frac{l}{t}\right)_{FC}\right] q_2 - \left[\frac{1}{A_3}\sum_3\left(\frac{l}{t}\right)\right] q_3 = \frac{1}{A_3}\sum_3 q'\left(\frac{l}{t}\right) \qquad (22a)$$

$$[2A_1] q_1 - [2A_2] q_2 - [2A_3] q_3 = \Sigma mq' + T_{EXT} \qquad (23a)$$

These equations are of the form:

$$Aq_1 - Bq_2 + Cq_3 = L \qquad (21b)$$

$$Dq_1 - Eq_2 - Fq_3 = M \qquad (22b)$$

$$-Gq_1 - Hq_2 - Kq_3 = N \qquad (23b)$$

Having the form of the necessary equations for the shear analysis and the algebraic values of the constants, attention is turned to the wing section to determine its properties. Figure 26 will aid in the understanding of symbols used in the tabular computations for numerical values of constants and shear flows. The tabular forms which follow represent a method for the orderly computation and methodical checking of numerical values.

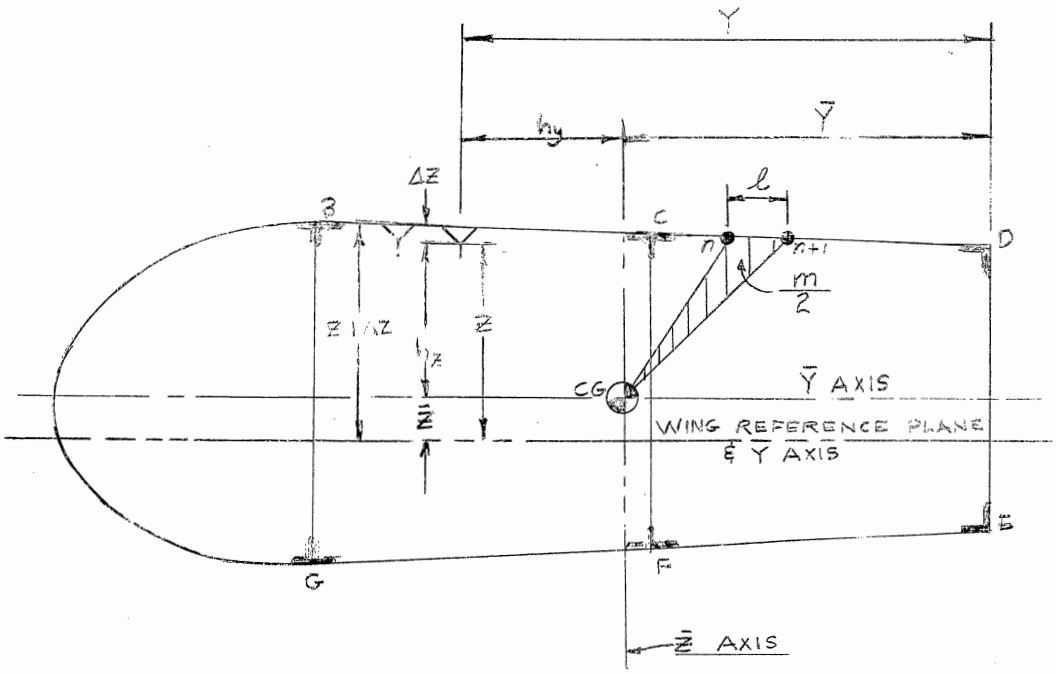

WING CROSS-SECTION

FIGURE 26

In TABLE II are found the computations for the wing section properties at station X_{RS} 273. This station location can be observed in Figure 25. The cross-section at this station consists of 4 spar caps and 41 stringers of the type shown in Figure 27. The large longitudinal beams extending from top to bottom of the cross-section are called spars, and the beam flanges are called spar caps. Computations have been shown for four stringers to illustrate the procedure used. In this example, the numbers 1 to 4 were arbitrarily assigned to the first four stringers toward the top of the section immediately aft of a vertical line through the C. G. of the section. These stringers are in cell 3. From an examination of Figure 24, and the data in TABLE II, it can be observed that the Y distances are measured with respect to the rear spar centerline E-D and the Z distances with respect to the wing reference plane, which is also the Y axis. Thus, using the rear spar and the wing reference plane as datum planes, the section properties are determined. The sign convention used is as follows:

Y-distances are negative when measured forward (toward the leading edge of the wing). Z-distances are negative when measured downward (toward the lower wing shell).

It may be noted in TABLE II that the area of part of the shell is included with the area of a stringer in the determination of the section properties. This has not been done in previous examples because of the assumption, which was then made, that no part of the shell resisted any bending moment. This assumption results in a simplification of computations for shear flows and the stringer loads and may often be justified, particularly in preliminary design or rough checking of a design. A more accurate analysis will show that the stringers of a thin-walled

TABLE II

WING SECTION PROPERTIES - STA. S_{RS} 273

$\bar{Y} = \frac{\Sigma AY}{\Sigma A} = \frac{\Sigma ④}{\Sigma ②} = -72.881$ (in.)

$\bar{Z} = \frac{\Sigma AZ}{\Sigma A} = \frac{\Sigma ⑦}{\Sigma ②} = 12.389$ (in.)

$I_z = \Sigma AY^2 - \bar{Y}\Sigma AY$

$= \Sigma ⑤ - \bar{Y}\Sigma ④$

$= 236,030$ (in.)^4

①	②	③	④	⑤	⑥	⑦	⑧
STRINGER	AREA OF SKIN-	Y	AY	AY^2	Z	AZ	AZ^2
No	STRINGER		② × ③	③ × ④		② × ⑥	⑥ × ⑦
1	2.674	-66.25	-177.153	11,736.38	31.778	84.974	2,700.3
2	2.674	-58.00	-155.092	8,995.34	31.142	83.274	2,593.3
3	2.674	-49.75	-133.032	6,618.34	30.413	81.324	2,473.3
4	2.674	-41.50	-110.971	4,605.30	29.574	79.081	2,338.7
Σ	111.798		-8147.897	828,030.0		1384.51	53,987.8

$I_y = \Sigma AZ^2 - \bar{Z}\Sigma AZ$

$= \Sigma ⑧ - \bar{Z}\Sigma ⑦$

$= 36,828$ (in.)^4

$I_{YZ} = \Sigma AYZ - \bar{Z}\bar{Y}\Sigma A$

$= \Sigma ⑨ - \bar{Z}\bar{Y}\Sigma ②$

$= -10,126$ (in.)^4

⑨	⑩	⑪	⑫	⑬	⑭	⑮	①
AYZ	ΔZ	Z + ΔZ	h_z	h_y	$h_z + \Delta z$	m	STRINGER
② × ③ × ⑥		⑥ + ⑩	⑥ - $\bar{Z}$	③ - $\bar{Y}$	⑫ + ⑩	$\frac{⑬_{n+1} \times ⑭_n}{+⑬_n \times ⑭_{n+1}}$	No
-5629.6	.439	32.217	19.389	6.631	19.828	167.80	1
-4829.9	.439	31.581	18.753	14.881	19.192	169.18	2
-4045.9	.439	30.852	18.024	23.131	18.463	171.73	3
-3281.9	.439	30.013	17.185	31.381	17.624	174.55	4
-110,070.9							

structure subjected to bending loads will transfer a portion of their loads to the metal shell to which they are attached. The metal shell will then act with the stringers to resist bending loads. Figure 27 is

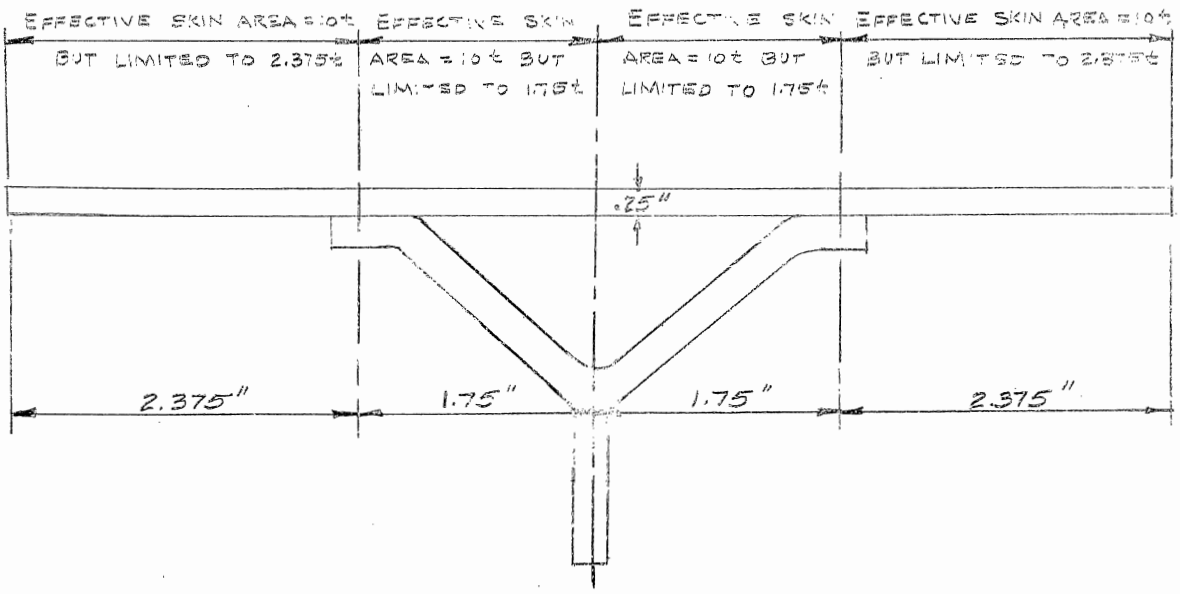

EFFECTIVE SKIN AREA

FIGURE 27

a sketch of a stringer and a portion of the shell of the airplane wing under examination in the present problem. From this sketch, it is seen that the designer has assumed an "effective area" of shell each side of a rivet line equal to 10 times the shell thickness to act with each stringer to resist bending loads. In most cases, the determination of the magnitude of this quantity is based on the judgement and experience

of the designer, often aided by test data and governed by specified limiting values and a desire for a quantity which affords ease in computation. It may be of interest to examine, briefly, the action of the stiffener-shell combination under load with a view to the determination of the effective area of shell which may be assumed to act with the stiffener to resist the imposed load.

Consider a 4 or 5 feet square panel consisting of a relatively thin metal sheet to which is attached a number of stringers placed parallel to each other. The dimensions of these structural components may be approximately those indicated in Figure 27. Assume the panel to be loaded in direct compression parallel to the longer axes of the stringers and prevented from column failure as a unit. Upon first loading, the stringers and shell will be equally stressed, but as loading progresses, the shell will begin to form a series of dish-shaped wrinkles about midway between stringers and extending the length of the panel. As these wrinkles form, the load will be gradually transferred from the wrinkled area toward the stringer, thereby loading the stringer and shell nearest the stringer heavier than the shell in the immediate vicinity of the wrinkles. Since very little additional load will be resisted by the shell in the vicinity of the wrinkles, the stringers and shell in close proximity will become more heavily stressed as loading progresses. If a curve of compressive stress in the panel be plotted as ordinates across the width of the panel, it would exhibit a minimum value at the wrinkled portion and a maximum over the stringers with intermediate values between these two points. Bruhn (1949) in his discussion of this subject states that it would not be feasible to use expressions for the actual stress distribution in the shell between stringers for design purposes because of their complexity.

To provide less complex formulas for use in design, attempts have been made to find expressions for an "effective width" or "effective area" of shell which would be assumed to act with the stiffener to resist load, be uniformly loaded with the same stress as that in the stringer, and be of such dimensions that the total load carried by this effective area would be equal to the total load in the shell between stringers. The shell material not included in this effective area would be assumed to be unstressed. Using the concept of effective areas of shell, then, the actual varied stress distribution across the panel will be replaced with a series of uniformly loaded stringer-shell combinations with portions of the shell in the vicinity of the wrinkles, between the stringers, carrying no load.

Let attention now be focused on a portion of the loaded panel consisting of two stringers and the intervening shell. If the sides of the shell are assumed to be simply supported at the stringer attachment, the rectangular shell tends to act as a series of square plates with wrinkles or buckles in each square, and Euler's formula for a flat plate can be used. (Peery, 1950).

$F_{c_{CR}} = \frac{\pi^2 E}{12(1-\mu^2)} \left(\frac{t}{L}\right)^2$ can be written

$F_{c_{CR}} = KE\left(\frac{t}{b}\right)^2$

where $F_{C_{CR}}$ is the total load on the panel section under consideration divided by the area bt of the shell between lines of attachment, t is the thickness of the shell, b is the width of the shell between attachment lines, L is the total length of the panel between loaded ends, and K is a function of $\left(\frac{L}{b}\right)$ and the degree of edge restraint. The value of K for various edge fixity conditions and $\left(\frac{L}{b}\right)$ ratios has been determined by experiment and results made readily made available. (Bruhn, 1949).

If the four edges of a long shell are considered simply supported, K is equal to 3.62 and

$$F_{c_{CR}} = 3.62\, E\left(\frac{t}{b}\right)^2$$

If the effective width of the shell each side of the stringer attachment line is w, and the total effective width of shell which acts with one stringer is 2w,

$$F_{c_{CR}} = K E\left(\frac{t}{2w}\right)^2$$

It was first proposed by Von Karman and Sechler to solve this equation for the effective width 2w in place of the shell width b when $F_{C_{CR}}$ was replaced by the yield point of the material (Bruhn, 1949). Since experiments have shown that the ultimate strength of the shell simply supported at the edges was independent of the width, the foregoing equation could be written as:

$$f_{yp} = 3.62\, E\left(\frac{t}{2w}\right)^2$$

where f_{yp} is the yield point of the material and 2w is the total effective width of the shell between the two stringers of the panel portion under consideration. Then:

$$w = .95\, t\sqrt{\frac{E}{f_{yp}}}$$

Later the yield point stress was replaced by the stiffener stress, f_{st}. Experimental work by Newell indicated that the value .95 was too high and should be replaced by .85 (Bruhn, 1949). The following equation has resulted and is widely used in aircraft practice:

$$w = .85\, t\sqrt{\frac{E}{f_{st}}}$$

The above equation is approximate when used for most thin-walled struc-

tures. If the stringers are stiff in torsion or, in other ways, do not let the shell edge rotate in the fashion of a simply supported one as assumed, the value of K will be greater than 3.62. Fischel's experiments indicate that for some shell-stiffener combinations common to aircraft construction, the edge conditions are more nearly clamped or fixed than simply supported, and K should be 6.35 as a minimum (Bruhn, 1949). However, the equation:

$$w = .85\, t \sqrt{\frac{E}{f_{st}}}$$

yields a smaller effective width than any other such expression proposed. It is conservative and considered satisfactory for design of normal aircraft structures. A more precise value may be desirable for very high speed aircraft whose wing shell thickness may be many times greater than that used on normal speed aircraft.

The solution to the above equation is a trial and error process with the values of f_{st} usually being assumed, w computed, and later corrected by a more accurate estimate of f_{st}. With reference to Figure 25, if f_{st} is estimated to be 10,500 pounds per square inch, w is 27t and the effective area as shown in the figure is approximately 7t. The quantity 10t was used for convenience in computations, and in view of the foregoing discussion, may be considered as satisfactory as the value of 7t computed.

With reference to equation (23a) it has been stated that twice the area connected with the determination of the shear flow q' from wing bending shall be designated by the symbol m. This area is listed in column 15 of TABLE II, and the method of computation shown in Figure 28. It may be noted that the arrangement of computations of this quan-

tity, and of others, affords ease of slide rule or desk calculator operation and adaptability to digital computers, such as the IBM TYPE 650.

SHOW THAT $m = bc - ad$ AS STATED IN COL. 15, TABLE II.

$$\frac{m}{2} = bc - \frac{cd}{2} - \frac{ab}{2} - \frac{(c-a)(b-d)}{2}$$

$$2\frac{m}{2} = bc - ad$$

$$\underline{m = bc - ad}$$

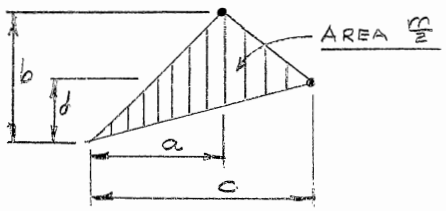

FIGURE 28

DETERMINATION OF AREA m

With the properties of the section determined, attention is turned to the computation of the stringer loads for which TABLE III is a suitable form. The wing is subjected to unsymmetrical bending. The general bending formula is used and is as follows:

$$f_b = \left[\frac{M_z I_y - M_y I_{yz}}{I_y I_z - I_{xy}^2}\right] h_y - \left[\frac{M_y I_z - M_z I_{yz}}{I_y I_z - I_{yz}^2}\right] h_z$$

where f_b is the bending stress in the stringer, M_Z and M_y are the bending moments about the Z and Y axes respectively, I_z and I_y are the moments of inertia about the X and Y axes respectively, and I_{yz} is the product of inertia. From Figure 25, it can be seen that:

$$M_z = 27{,}000(500-72) = 11.556 \times 10^6 \text{ in.-lbs.}$$

$$M_y = 200{,}000(500-72) = 85.6 \times 10^6 \text{ in.-lbs}$$

The moments of inertia and products of inertia have been computed in TABLE II. The loads P in the stringers are computed as the bending stress multiplied by the effective area of the stringer-skin combination.

TABLE III

SKIN-STRINGER ELEMENT STRESSES AND LOADS - STA. X_{RS} 273

$K_1 = -\left[\frac{M_z I_y - M_y I_{yz}}{I_y I_z - I_{yz}^2}\right] = -150.451$ $\quad K_2 = -\left[\frac{M_y I_z - M_z I_{yz}}{I_y I_z - I_{yz}^2}\right] = -2365.686$

$M_y = 85.6 \times 10^6$ in.-lbs. $\quad M_z = 11.556 \times 10^6$ in.-lbs

(1)	(2)	(3)	(4)	(5)	(6)	(7)
Stringer No.	h_y Col. (13) Table II	h_z Col. (12) Table II	$K_1 h_y$ $K_1 \times$ (2)	$K_2 h_z$ $K_2 \times$ (3)	f_b (4) + (5)	P (6) x (2) Table II
1	6.631	19.389	-998	-45 868	-46 866	-125 320
2	14.881	18.753	-2239	-44 364	-46 603	-124 6[illegible]
3	23.131	18.024	-3480	-42 639	-46 119	-123 3[illegible]
4	31.381	17.185	-4721	-40 654	-45 375	-121 3[illegible]
Σ						

In the same manner, the section properties of the next two adjacent wing sections are computed, and the stringer loads found. The results are shown in TABLES IV, V, VI and VII which follow.

TABLE IV

WING SECTION PROPERTIES - STA. X_{RS} 237

$\bar{Y} = -75.317$ in. $\bar{Z} = 14.357$ in. $I_z = 266,900$ $(in)^4$

(1)	(2)	(3)	(4)	(5)	(6)	(7)	(8)
STRINGER	AREA OF SKIN-	Y	AY	AY^2	Z	AZ	AZ^2
No	STRINGER		(2) x (3)	(3) x (4)		(2) x (6)	(6) x (7)
1	2.817	-66.25	-186.626	12,363.9	34.129	96.7	3281.7
2	2.817	-58.00	-163.386	9,476.39	33.154	94.0	3125.0
3	2.817	-42.15	-140.146	6,972.26	32.681	92.1	3008.6
4	2.817	-41.50	-116.906	4,821.60	31.809	89.8	2850.0

$I_y = 42,694.85$ $(in)^4$ $I_{yz} = -12,399.493$

(9)	(10)	(11)	(12)	(13)	(14)	(15)	(1)
AYZ	Δz	$z+\Delta z$	h_z	h_y	$h_z+\Delta z$	m	STRINGER
(2) x (3) x (6)		(6) + (10)	(6) - $\bar{z}$	(3) - $\bar{Y}$	(12) + (10)	$(13)_{n+1} \times (14)_n - (13)_n \times (14)_{n+1}$	No.
-6369.36	.431	34.560	19.772	7.067	20.203	172.822	1
-5665.43	.431	33.585	18.794	17.317	19.225	174.415	2
-4090.11	.431	33.112	18.324	23.167	18.755	177.023	3
-3718.66	.431	32.240	17.452	33.817	17.883	180.067	4

TABLE V

SKIN-STRINGER ELEMENT STRESSES AND LOADS - STA. X_{RS} 237

$K_1 = -149.14$ $\qquad$ $K_2 = -2217.11$

$M_y = 92.8 \times 10^6$ in.-lbs $\qquad$ $M_z = 12.538 \times 10^6$ in-lbs

(1)	(2)	(3)	(4)	(5)	(6)	(7)
STRINGER	h_y	h_z	$K_1 h_y$	$K_2 h_z$	f_b	P
No	COL (13) TABLE IV	COL (12) TABLE IV	$K_1 \times$ (2)	$K_2 \times$ (3)	(4)+(5)	(6)+(2) TABLE IV
1	9.067	19.772	-1360	-43,836	-45,196	-123,317
2	17.317	18.794	-2597	-41,333	-44,930	-126,562
3	23.167	18.324	-3834	-40,626	-44,460	-125,244
4	33.817	17.452	-5071	-38,693	-43,764	-123,283

TABLE VI

WING SECTION PROPERTIES - STA. X_{RS} 201

$\bar{Y} = -74.648$ in. $\quad \bar{Z} = 16.215$ in. $\quad I_z = 306,559$ $(in)^4$

(1)	(2)	(3)	(4)	(5)	(6)	(7)	(8)
STRINGER No.	AREA OF SKIN - STRINGER	Y	AY (2) x (3)	AY^2 (3) x (4)	Z	AZ (2) x (6)	AZ^2 (6) x (7)
1	3.076	-66.25	-203.785	13,501	36.402	111.973	4076.
2	3.076	-58.00	-178.408	10,348	35.682	109.758	3916.
3	3.076	-49.75	-153.031	7,613	34.877	107.282	3742.
4	3.076	-41.50	-127.654	5,298	33.968	104.486	3549.

$I_y = 50,146$ $(in.)^4$ $\quad I_{yz} = -15,170.3$ $(in.)^4$

(9)	(10)	(11)	(12)	(13)	(14)	(15)	(1)
AYZ (2) x (3) x (6)	Δz	$z + \Delta z$ (6) + (10)	h_z (6) - $\bar{z}$	h_y (3) - $\bar{y}$	$h_z + \Delta z$ (12) + (10)	m $(13)_{n+1} \times (14)_n + (13)_n \times (14)_{n+1}$	STRINGER No.
-7418.18	.489	36.891	20.187	11.398	20.676	178.784	1
-6365.95	.489	36.171	19.467	19.648	19.956	182.418	2
-5337.26	.489	35.366	18.662	27.898	19.151	183.353	3
-4336.15	.489	34.457	17.753	36.148	18.242	186.355	4

TABLE VII

SKIN-STRINGER ELEMENT STRESSES AND LOADS - STA. X_{RS} 201

$K_1 = -144.8896$ $\quad K_2 = -2,038$

$M_y = 100 \times 10^6$ in.-lbs $\quad M_z = 13.5 \times 10^6$ in.-lbs

①	②	③	④	⑤	⑥	⑦
STRINGER No	h_y COL 13 TABLE VI	h_z COL. 12 TABLE VI	$K_1 h_y$ $K_1 \times 2$	$K_2 h_z$ $K_2 \times 3$	f_b 4 + 5	P 6 x 2 TABLE VI
1	11.398	20.187	-1651.45	-41,141.11	-42,792.56	-131,629.9
2	19.648	19.467	-2846.79	-39,673.75	-42,520.54	-130,793.2
3	27.898	18.662	-4042.13	-38,033.16	-42,075.29	-129,423.6
4	36.148	17.753	-5237.47	-36,180.61	-41,418.08	-127,402.0

The wing section properties and stringer loads have been computed in TABLES II to VII for three cross-sections, each thirty-six inches from the other. The cross-section at which the shear flows are desired is the center one of the three. The information contained in TABLES II to VII is a necessary prerequisite to the completion of TABLE VIII which contains the required shear flows at STA. X_{RS} 237. An examination of the information of TABLE VIII will now be made.

All columns of TABLE VIII, with the exception of column 15, may be completed using previous computations and information from the geometry of the structure. The change in load on a stringer, ΔP, is calculated as the difference between loads at the two extreme cross-sections, X_{RS} 273 and 201. (X_{RS} indicates a distance along the rear spar of the wing from

TABLE VIII

WING SHEAR FLOWS AT STA. X_{RS} 237

$A_1 = 1175\ (in)^2$ $\quad A_2 = 2782\ (in)^2$ $\quad A_3 = 3158\ (in)^2$

$q_1 = 418\ lbs/in.$ $\quad q_2 = 169\ lbs/in$ $\quad q_3 = -724\ lbs/in$

(1)	(2)	(3)	(4)	(5)	(6)	(7)	(8)
STRINGER No	$P_{STA\ 201}$ COL (7) TABLE VII	$P_{STA\ 273}$ COL (9) TABLE III	ΔP (2) - (3)	$\Sigma q'$ Σ(4)/(273-201)	m COL (15) TABLE IV	$\Sigma mq'$ (5) x (6)	ℓ
1	-131,630	-125,320	- 6310				
				2413.36	177.822	429,082	8.25
2	-130,793	-124,616	- 6177				
				2499.15	174.415	435,889	8.25
3	-129,424	-123,322	- 6102				
				2583.7	177.013	457,410	8.25
4	-127,402	-121,333	- 6069				
				2668.19	180.663	480,453	8.25

(9)	(10)	(11)	(12)	(13)	(14)	(15)	(1)
t	$(\frac{\ell}{t})$ CELL 1	$(\frac{\ell}{t})$ CELL 2	$(\frac{\ell}{t})$ CELL 3	$q'(\frac{\ell}{t})$ CELL 2	$q'(\frac{\ell}{t})$ CELL 3	q NET	STRINGER
	(8)/(9)	(8)/(9)	(8)/(9)	(5) x (11)	(5) x (13)	(5) + q	No
.244	—	—	33.811	—	81,598	1689.36	1
.244	—	—	33.811	—	84,449	1775.15	2
.244	—	—	33.811	—	87,364	1859.9	3
.244	—	—	33.811	—	90,214	1944.19	4

a selected origin which may be located in the vertical plane of symmetry of the airplane.) The shear flows in the wing shell are found at the intermediate cross-section, STA. X_{RS} 237. Hense, the quantities M, ℓ , and t are those at this station. The values of the shear flows found are assumed to be constant between the two extreme cross-sections. The quantities A_1, A_2, and A_3 are found from the geometry of the cross-section as the areas enclosed by the perimeters of cell 1, cell 2 and cell 3, respectively. For NACA airfoil sections or company standards, the total area enclosed by the airfoil shell is usually readily available.

In column 15 is found the shear flows, q_{NET}, between stringers. q_{NET} is the result of the algebraic addition of q', the relative shear flows from wing bending, and q_1, and q_2, or q_3, depending on which cell is under consideration. The values of q' are found in TABLE VIII but q_1, q_2, and q_3 will be unknown at the time this table is filled out. The simultaneous solution of equations (21a), (22a), and (23a), whose constants are arranged conveniently in TABLE IX, yields these quantities. q_1, q_2, and q_3 thus found are shown at the top of TABLE VIII and q_{NET} recorded in column 15.

TABLE IX

CONSTANTS OF SHEAR FLOW EQUATIONS (21a), (22a), (23a)

CONSTANT	ALGEBRAIC FORM	TABULAR QUANTITIES (TABLE VIII)	NUMERICAL FORM	RESULT
A	$\frac{1}{A_1}\sum_1\left(\frac{l}{t}\right)+\frac{1}{A_2}\left(\frac{l}{t}\right)_{GB}$	$\frac{\Sigma \text{ COL } 10}{A_1}+\frac{1}{A_2}\left(\frac{l}{t}\right)_{GB}$	$\frac{1534.786}{1175}+\frac{249.786}{2782}$	1.3959
B	$\frac{1}{A_2}\sum_2\left(\frac{l}{t}\right)+\frac{1}{A_1}\left(\frac{l}{t}\right)_{GB}$	$\frac{\Sigma \text{ COL } 11}{A_2}+\frac{1}{A_1}\left(\frac{l}{t}\right)_{GB}$	$\frac{1123.98}{2782}+\frac{249.786}{1175}$	.6166
C	$\frac{1}{A_2}\left(\frac{l}{t}\right)_{FC}$		$\frac{295.929}{2782}$	.10637
D	$\frac{1}{A_1}\sum_1\left(\frac{l}{t}\right)$	$\frac{\Sigma \text{ COL } 10}{A_1}$	$\frac{1534.786}{1175}$	1.3062
E	$\frac{1}{A_1}\left(\frac{l}{t}\right)_{GB}-\frac{1}{A_3}\left(\frac{l}{t}\right)_{FC}$		$\frac{249.786}{1175}-\frac{295.929}{3158}$	.11887
F	$\frac{1}{A_3}\sum_3\left(\frac{l}{t}\right)$	$\frac{\Sigma \text{ COL } 12}{A_3}$	$\frac{1231.887}{3158}$	.3901
G	$2A_1$		2×1175	2350.0
H	$2A_2$		2×2782	5564.0
K	$2A_3$		2×3158	6316.0
L	$\frac{1}{A_2}\sum_2 g'\left(\frac{l}{t}\right)$	$\frac{\Sigma \text{ COL } 13}{A_2}$	$\frac{1.1223 \times 10^6}{2782}$	403.422
M	$\frac{1}{A_3}\sum_3 g'\left(\frac{l}{t}\right)$	$\frac{\Sigma \text{ COL } 14}{A_3}$	$\frac{2.5578 \times 10^6}{3158}$	809.947
N	$\Sigma m g' + T_{EXT}$	COL 7 + T_{EXT}	$(22.6496-20)\times 10^6$	2.6496×10^6

TABLE IX

CONSTANTS OF SHEAR FLOW EQUATIONS (21a), (22a), (23a)

CONSTANT	ALGEBRAIC FORM	TABULAR QUANTITIES (TABLE VIII)	NUMERICAL FORM	RESULT
A	$\frac{1}{A_1}\sum_1\left(\frac{l}{t}\right)+\frac{1}{A_2}\left(\frac{l}{t}\right)_{GB}$	$\frac{\Sigma \text{ COL } 10}{A_1}+\frac{1}{A_2}\left(\frac{l}{t}\right)_{GB}$	$\frac{1534.786}{1175}+\frac{249.786}{2782}$	1.3959
B	$\frac{1}{A_2}\sum_2\left(\frac{l}{t}\right)+\frac{1}{A_1}\left(\frac{l}{t}\right)_{GB}$	$\frac{\Sigma \text{ COL } 11}{A_2}+\frac{1}{A_1}\left(\frac{l}{t}\right)_{GB}$	$\frac{1123.98}{2782}+\frac{249.786}{1175}$	.6166
C	$\frac{1}{A_2}\left(\frac{l}{t}\right)_{FC}$		$\frac{295.929}{2782}$	.10637
D	$\frac{1}{A_1}\sum_1\left(\frac{l}{t}\right)$	$\frac{\Sigma \text{ COL } 10}{A_1}$	$\frac{1534.786}{1175}$	1.3062
E	$\frac{1}{A_1}\left(\frac{l}{t}\right)_{GB}-\frac{1}{A_3}\left(\frac{l}{t}\right)_{FC}$		$\frac{249.786}{1175}-\frac{295.929}{3158}$	.11887
F	$\frac{1}{A_3}\sum_3\left(\frac{l}{t}\right)$	$\frac{\Sigma \text{ COL } 12}{A_3}$	$\frac{1231.887}{3158}$	.3901
G	$2A_1$		2×1175	2350.0
H	$2A_2$		2×2782	5564.0
K	$2A_3$		2×3158	6316.0
L	$\frac{1}{A_2}\sum_2 g'\left(\frac{l}{t}\right)$	$\frac{\Sigma \text{ COL } 13}{A_2}$	$\frac{1.1223 \times 10^6}{2782}$	403.422
M	$\frac{1}{A_3}\sum_3 g'\left(\frac{l}{t}\right)$	$\frac{\Sigma \text{ COL } 14}{A_3}$	$\frac{2.5578 \times 10^6}{3158}$	809.947
N	$\Sigma m g' + T_{EXT}$	COL 7 + T_{EXT}	$(22.6496-20)\times 10^6$	2.6496×10^6

TABLE IX

CONSTANTS OF SHEAR FLOW EQUATIONS (21a), (22a), (23a)

CONSTANT	ALGEBRAIC FORM	TABULAR QUANTITIES (TABLE VIII)	NUMERICAL FORM	RESULT
A	$\frac{1}{A_1}\sum_1\left(\frac{l}{t}\right)+\frac{1}{A_2}\left(\frac{l}{t}\right)_{GB}$	$\frac{\Sigma \text{ COL } 10}{A_1}+\frac{1}{A_2}\left(\frac{l}{t}\right)_{GB}$	$\frac{1534.786}{1175}+\frac{249.786}{2782}$	1.3959
B	$\frac{1}{A_2}\sum_2\left(\frac{l}{t}\right)+\frac{1}{A_1}\left(\frac{l}{t}\right)_{GB}$	$\frac{\Sigma \text{ COL } 11}{A_2}+\frac{1}{A_1}\left(\frac{l}{t}\right)_{GB}$	$\frac{1123.98}{2782}+\frac{249.786}{1175}$	.6166
C	$\frac{1}{A_2}\left(\frac{l}{t}\right)_{FC}$		$\frac{295.929}{2782}$	.10637
D	$\frac{1}{A_1}\sum_1\left(\frac{l}{t}\right)$	$\frac{\Sigma \text{ COL } 10}{A_1}$	$\frac{1534.786}{1175}$	1.3062
E	$\frac{1}{A_1}\left(\frac{l}{t}\right)_{GB}-\frac{1}{A_3}\left(\frac{l}{t}\right)_{FC}$		$\frac{249.786}{1175}-\frac{295.929}{3158}$	.11887
F	$\frac{1}{A_3}\sum_3\left(\frac{l}{t}\right)$	$\frac{\Sigma \text{ COL } 12}{A_3}$	$\frac{1231.887}{3158}$	.3901
G	$2A_1$		2×1175	2350.0
H	$2A_2$		2×2782	5564.0
K	$2A_3$		2×3158	6316.0
L	$\frac{1}{A_2}\sum_2 g'\left(\frac{l}{t}\right)$	$\frac{\Sigma \text{ COL } 13}{A_2}$	$\frac{1.1223 \times 10^6}{2782}$	403.422
M	$\frac{1}{A_3}\sum_3 g'\left(\frac{l}{t}\right)$	$\frac{\Sigma \text{ COL } 14}{A_3}$	$\frac{2.5578 \times 10^6}{3158}$	809.947
N	$\Sigma m g' + T_{EXT}$	COL 7 + T_{EXT}	$(22.6496-20)\times 10^6$	2.6496×10^6

PART XI

CONCLUSIONS AND RECOMMENDATIONS

The problem in this report has been to accumulate information on the basic theories and analytical tools used for the determination of the shearing stresses in thin-walled, multi-cell, multi-stiffener structures and to formulate procedures for the shear analysis of these structures. Most of the basic theories have been gathered from text books about aircraft structures, such as Bruhn (1949) and Peery (1950) and text books regarding mechanics of materials, such as Seeley (1955) and Timoshenko (1956). The information so gathered and illustrated in this report builds into a procedure for the shear analysis of a complicated multi-cell, multi-stiffener, thin-walled structure in the form of an airplane wing. This procedure, shown and explained in PART X of this report, is especially useful for applicable structures whose boundary surfaces cannot be expressed in easily manipulated mathematical expressions. The arrangement and grouping of the tabular computations of the procedure shown in PART X is such that digital computers, such as the IBM TYPE 650, may be used for the problem solution with a minimum of effort expended in transposing and rearranging data.

Many publications regarding the results of research and testing programs for the structures with which this report is concerned are available from such governmental agencies as the National Advisory Committee for Aeronautics, Washington, D. C. However, these research and testing

programs have for their ultimate aim the examination of the behavior of the structure at or near failure. Hense, little information regarding basic theory of shear analysis will be found in these documents. An examination of the data curves, graphs, and photograph reproductions of tested structures will acquaint the reader with the nature and behavior of these structures under load. For example, the effect of varying distances between stiffeners on the point at which inelastic behavior occurs can be observed.

Regarding thin-walled structures, it can be said that a multitude of subjects for future study present themselves. Fortunately, a large amount of printed matter is available in the form of books, research and testing reports, and publications of the engineering societies. A source of knowledge not to be overlooked is found in the persons of those qualified engineers who are willing to teach those students who are willing to learn. The following pattern for future study is recommended.

1. Discover if the procedures outlined in this report for the shear analysis of multi-cell, multi-stiffener, thin-walled structures can be improved so as to result in a more accurate analysis, with less effort, and particularly with a saving of weight for the structure involved.

2. Determine the effect of stress concentrations around openings, or "cut-outs," in the shell and of the close proximity of a longitudinal or transverse stiffener on the shear stresses in the shell.

3. Study the effect on procedures outlined in this report when the thickness of the shell increases to the proportions found on some of the present high speed aircraft.

SELECTED BIBLIOGRAPHY

Bruhn, E. F. Analysis and Design of Airplane Structures. Cincinnati, Ohio: Tri-State Offset Co., 1949

Clark, J. W. and R. L. Moore. Torsion Tests of Aluminum Alloy Stiffened Circular Cylinders. Washington, D. C.: National Advisory Committee for Aeronautics, NACA TN 2821, 1952

Lunquist, E. E. Strength Tests on Thin-Walled Duralumin Cylinders in Torsion. Langley Field, Virginia: Langley Memorial Aeronautical Laboratory, NACA TN 427, 1932

Lunquist, E. E. Strength Tests of Thin-Walled Duralumin Cylinders in Combined Transverse Shear and Bending. Washington, D. C.: National Advisory Committee for Aeronautics, NACA TN 523, 1935

Lunquist, E. E. and W. F. Burke. Strength Tests of Duralumin Cylinders of Elliptical Section. Langley Field, Virginia: Langley Memorial Aeronautical Laboratory, NACA TN 527, 1935

Peery, D. J. Aircraft Structures. New York, N. Y.: McGraw-Hill Book Co., Inc., 1950

Schapitz, E. The Twisting of Thin-Walled, Stiffened Circular Cylinders. Washington, D. C.: National Advisory Committee for Aeronautics, NACA TN 878, 1938

Seely, F. B. and J. O. Smith. Advanced Mechanics of Materials. New York, N. Y.: John Wiley and Sons, Inc., 1955

Timoshenko, S. Strength of Materials. PART II. New York, N. Y.: D. Van Nostrand Co., Inc., 1956

Unpublished data and information received from Douglas Aircraft Co., Inc., Tulsa Division, Tulsa, Oklahoma.

VITA

JOHN J. REID

Candidate for the degree of

Master of Science

TITLE: PROCEDURE FOR THE SHEAR ANALYSIS OF THIN-WALLED METAL CYLINDERS SUBJECTED TO BENDING AND TORSIONAL LOADS

MAJOR: Civil Engineering (Structural Analysis)

Biographical

Personal data: Born April 13, 1921 in Magherafelt, Ireland.

Education: Received Bachelor of Science degree in Civil Engineering from the University of New Mexico, Albuquerque, New Mexico in June, 1951; undertook graduate study at University of New Mexico, Tulsa University, Tulsa, Oklahoma, and completed requirements for the Master of Science degree at Oklahoma State University, Stillwater, Oklahoma in August, 1957.

Professional Experience: United States Army, 1942-1946, Infantry Officer; U. S. Army Corps of Engineers, Albuquerque, New Mexico, 1951-1952, Construction Engineer; Sandia Corporation, New Mexico, 1952-1953, Mechanical Engineer; Douglas Aircraft Co., Santa Monica, California, 1953-1954, Tool Engineer; Lee C. Moore Corporation, Tulsa, Oklahoma, 1954-1955, Structural Engineer; Douglas Aircraft Co., Tulsa, Oklahoma, 1955-1956, Stress Analyst.

Member of Sigma Tau and Chi Epsilon engineering honorary societies.